

Ciprofloxacin removal from aqueous media by adsorption process: a systematic review and meta-analysis

Mahshid Malakootian^a, Maryam Faraji^{b,c}, Mohammad Malakootian^{b,c}, Majid Nozari^{b,c,*}

^aCardiogenetic Research Center, Rajaie Cardiovascular Medical and Research Center, Iran University of Medical Sciences, Tehran, Iran, email: Malakootian@rhc.ac.ir

^bEnvironmental Health Engineering Research Center, Kerman University of Medical Sciences, Kerman, Iran

^cDepartment of Environmental Health Engineering, Faculty of Public Health, Kerman University of Medical Sciences, Kerman, Iran, Tel. +98-9383921819; emails: nozari.m@kmu.ac.ir (M. Nozari), m.faraji@kmu.ac.ir/m_faraji28@yahoo.com (M. Faraji), m.malakootian@yahoo.com (M. Malakootian)

Received 28 January 2021; Accepted 16 April 2021

ABSTRACT

In this study, the adsorption of ciprofloxacin was reviewed from aqueous media (water and wastewater) in studies published over the last years (1990–2020). The objective of this research was to analyze ciprofloxacin removal from aqueous media by adsorption process through a systematic review and meta-analysis. It was found that the ciprofloxacin adsorption data were well fitted on the Langmuir isotherm and the pseudo-second-order kinetic models. The review further showed that the optimum pH ranged from 6 to 8.5 in most articles. Based on the reported results, the temperature and standard enthalpy change (ΔH°) varied in the range of 273–388 K and -1,212.6 to 170.21 kJ/mol, respectively. The maximum reported adsorption capacity for ciprofloxacin was 1,575 mg/g for C@silica core/shell nanoparticles. Also, the minimum adsorption capacity was related to birnessite (47 ng/g). The most effective adsorbent for ciprofloxacin removal was C@silica core/shell nanoparticles from ZIF-8. The results of the meta-analysis revealed that the adsorption process could remove ciprofloxacin with an acceptable mean efficiency of 59.32% (95% CI: 44.66–73.97). It can be suggested to apply the novel hybrid processes, adsorbent modification, composite adsorbent development, neural network modeling to increase ciprofloxacin adsorption.

Keywords: Ciprofloxacin; Adsorption; Aqueous solution; Systemic review; Meta-analysis

1. Introduction

Population growth and increased production and consumption of emerging pollutants have destroyed the quality of water resources. The amount and types of these hazardous pollutants and related problems are increasing. They can cause enzymatic, hormonal, and genetic disorders in humans [1–5]. Recent researches have reported a large number of emerging pollutants, the metabolites of which have been identified in aqueous media. Conventional water and effluent treatment methods, including physical, chemical,

and biological processes (individually or in combination) cannot remove or degrade these pollutants such that most of them eventually enter the ecosystem [6,7]. Antibiotics are among the emerging pollutants that can cause severe impact effects if their residues enter the body [8]. They target certain responsible organisms and destroy ecosystems. Some of them are non-biodegradable and remain in the environment for a long time [9,10]. Ciprofloxacin like other antibiotics could accumulate in the body of organisms, thus posing a potential health risk. Therefore, due to the high-level concentration in various wastewaters, stability, resistance to

* Corresponding author.

degradation, and potential ecotoxicity, the effective removal of ciprofloxacin is plausible [11–14].

Ciprofloxacin is one of the most important antibiotics in medicine for the treatment of bacterial infections caused by Gram-positive and Gram-negative bacteria [15]. Ciprofloxacin concentrations were reported to be 0.001 mg/L in effluent and surface water, more than 0.15 mg/L in hospital wastewater, and 30 mg/L in pharmaceutical wastewater [16]. Although the concentration of ciprofloxacin may be low in aqueous media, its continued accumulation can increase the potential hazards to aquatic ecosystems as well as concerns about its biological and genetic damages [17,18]. Ciprofloxacin has a high solubility in aqueous media and high sustainability in soil and effluent systems at different pH conditions [19]. Several physicochemical processes have been used to remove ciprofloxacin from aqueous media such as ozonation [20], photocatalytic processes [21–23], adsorption [24,25], Fenton, and electrocoagulation [26,27].

There are many concerns about the presence of antibiotics, including ciprofloxacin in the surface and drinking water, because they can pose a potential threat to the environment and human health. Chronic toxicity, endocrine disruption, and direct toxicity of microflora, even at low concentrations, are among these concerns [27]. This study aimed to review papers on the adsorption of ciprofloxacin from different aqueous media from 1990 to 2020 to determine which aqueous media, by what adsorbents, and to what efficiency can adsorb this antibiotic. In addition, the meta-analysis of the results of some papers determined the mean ciprofloxacin adsorption efficiency. The results of the current study will help researchers to identify shortcomings, and conduct their future studies on efficient processes and fill the gap of knowledge.

2. Materials and methods

This review study was conducted during the second six months of 2019 and the first month of 2020. The research team was composed of four university professors who were interested in the subject of study and had research backgrounds in the various fields of research. The members of this team collaborated by supervising the research, monitoring the work process, extracting and data.

2.1. Literature sources and search strategies

The papers analyzed in this study were those published from 1990 to 2020. An extensive search was conducted on the electronic information sources of PubMed (1 October 2019 to 30 October 2019), Web of Science (1 November 2019 to 06 December 2019), Proquest (7 December 2019 to 24 December 2019), and Scopus (25 December 2019 to 30 December 2019) based on the following terms (using the Medical Subject Headings (MeSH)): ((Organic material) OR (Micropollutant)) AND ((Drug) OR (Fluoroquinolone) OR (Pharmaceutical) OR ((Antibiotic) OR (Ciprofloxacin)) AND ((Degradation) OR Adsorption) OR (Removal) OR (Mineralization) OR (Decomposition) OR (Oxidation) OR (Treatment) OR (Abatement) OR (Elimination)) AND ((Aqueous) OR (Seawater) OR (Groundwater) OR (Water) OR (Freshwater) OR (Wastewater) OR (Waste) OR (Effluent) OR (Influent)).

2.2. Inclusion and exclusion criteria

The literature search was limited to peer-reviewed publications written in English between 1990 until January 2020. After this stage, we considered a set of inclusion and exclusion criteria, which are described below:

The study inclusion criteria apply to each publication, which consists of scope (Step 1), study quality (Step 2), and data availability (Step 3). For Step 1, two independent screeners first evaluated the titles and abstracts of the retrieved articles to assess whether the paper included ciprofloxacin removal using the adsorption process in aqueous media. In addition, the full text of the papers whose abstracts passed the first screening step to confirm that the document contained an experimental study and to evaluate the efficiency of the ciprofloxacin adsorption process. We excluded books, presentations, review papers, and letters to the editor about the adsorption process for the removal of ciprofloxacin and other environmental matrices such as soil and air. Also, papers about the development of detection methods of ciprofloxacin in different media were excluded. Information on each paper was extracted, such as the first author, year of publication, the type and nature of the adsorbent, initial concentration, fitted models, thermodynamic parameters, optimum pH, adsorption capacity and removal efficiency. For Step 2, the quality of a study was evaluated independently by two scientific reviewers. The studies have passed the criteria of clarity. Publications in which their study and associated methodologies were not sufficiently documented to investigate the quality of the study were not included. After a publication passed both scope and quality criteria, the availability of the data (Step 3) was analyzed. For this selection step, papers that used the experimental design method were included in the meta-analysis

2.3. Meta-analysis

Papers with accessible experimental data were included in the meta-analysis. Eventually, 8 papers were meta-analyzed. The binomial distribution was applied to calculate the variance of the data in each paper. Cochran test and I^2 index were used to evaluate the heterogeneity of data, and the random-effects model was used to combine papers due to the heterogeneity in them. Data were analyzed using STATA software (version 12.2). A P -value of less than 0.05 was considered as the significant level.

3. Results

The PRISMA flow diagram (the flow diagram depicts the flow of information through the different phases of a systematic review) for the inclusion of studies in the systematic review is shown in Fig. 1. The extracted data from selected papers about the adsorption of ciprofloxacin from water and wastewater media are shown in Tables 1 and 2, respectively. The classification of published papers on ciprofloxacin adsorption based on the type of media and adsorbent as illustrated in Fig. 2a and b, respectively. Fig. 3 shows the number of relevant publications from 1990 to 2020. A forest plot of the mean efficiencies of

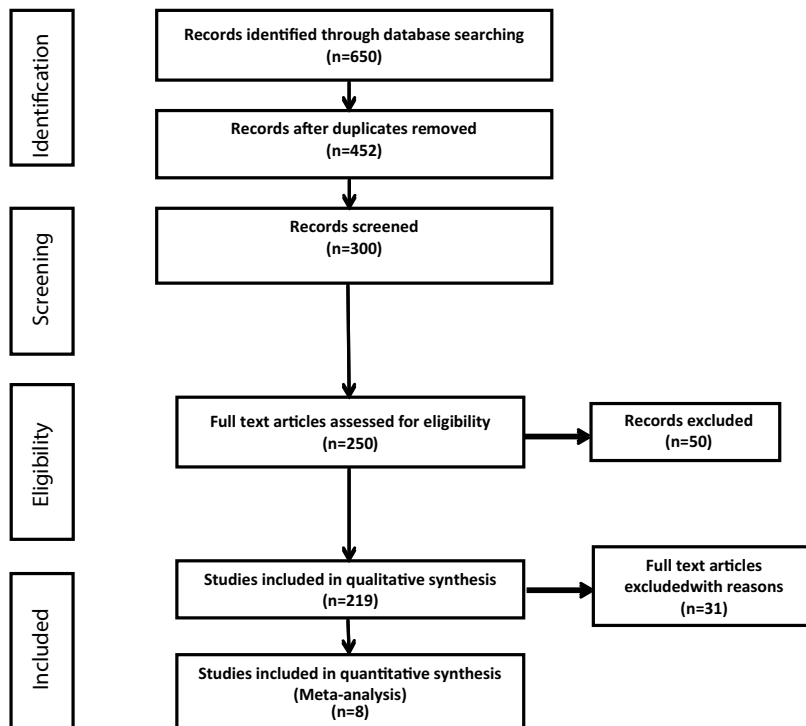


Fig. 1. PRISMA flow diagram for the inclusion of studies in the systematic review.

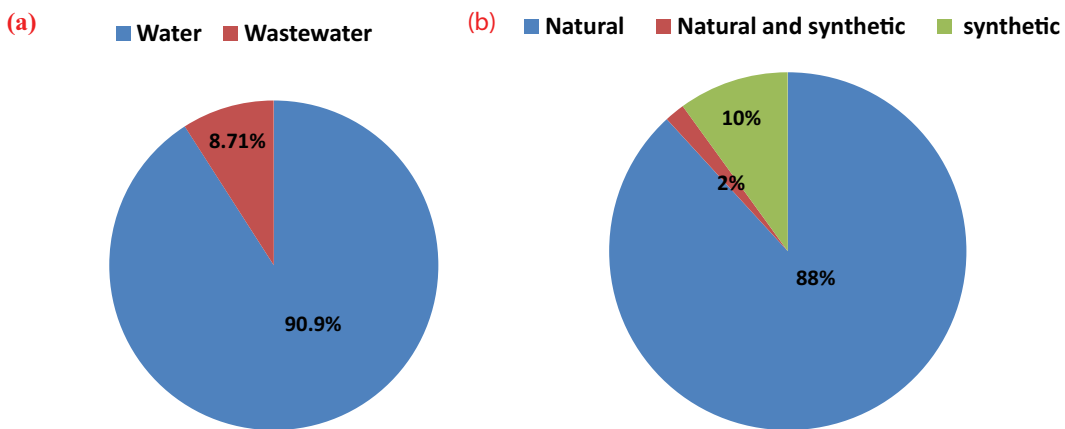


Fig. 2. Classification of published papers on ciprofloxacin adsorption based on (a) the type of aquatic environment (water or wastewater) and (b) the type of adsorbent nature (natural, synthetic or natural and synthetic).

ciprofloxacin removal by the adsorption process is demonstrated in Fig. 4. Experimental conditions of the studies included in the meta-analysis shown in Table 3.

4. Discussion

This study aimed to investigate the removal of ciprofloxacin from two aqueous media (water and wastewater) by adsorption process, through a systematic review and meta-analysis. From 219 papers reviewed, 199 (90.9%) and 20 (9.13%) papers survived the removal efficiency of ciprofloxacin in water and wastewater media, respectively

(Fig. 2a). As shown in Fig. 3, no paper has been published on the ciprofloxacin removal from aqueous media until 2008 and less than 10 papers have been published from 2009 to 2013. The number of published papers has increased from 2014 to 2019 so that the highest number of papers was published in 2019 (64 papers). An increasing trend in published papers from 1990 to 2020 could be associated with several factors; further usage of antibiotics in recent years, the establishment of strict standards on the quality of drinking water and water bodies, improvement of the analytical chemistry, and more researches about the impact effects of emerging pollutants on the human health and ecosystems.

Table 1
Adsorption processes applied with different adsorbents to adsorb ciprofloxacin from water media resulting from papers published from 1990 to 2020 (the type and nature of the adsorbent, initial concentration (mg/L), fitted models (kinetics and isotherms), thermodynamic parameters (T ($^{\circ}\text{K}$), ΔH° (kJ/mol)), optimum pH, adsorption capacity (mg/g), and removal efficiency (%))

No.	Adsorbent	Adsorbent type (natural or synthetic)	Initial Concentration (mg/L)	Fitted model		Thermodynamic			Optimum Adsorption capacity/ pH	Unit	References	
				Kinetics	Isotherms	T ($^{\circ}\text{K}$)	ΔH° (kJ/mol)	Type of process	E_a (kJ/mol)			
1	Synthesized nanoceria	Synthetic	200	Pseudo-first-order and pseudo-second-order	Freundlich	298–318	-1,212.6	Exothermic	Physical and chemical	5	49.3	mg/g [28]
2	Bentonite	Natural	50–500	Pseudo-first-order	Langmuir	—	—	—	—	4.5	147.0	mg/g [29]
3	Chitosan grafted $\text{SiO}_2\text{-Fe}_3\text{O}_4$ nanoparticles	Synthetic	5–40	Pseudo-second-order	Langmuir	—	—	—	—	12	100.7	mg/g [30]
4	Zinc oxide supported on SBA-15 type mesoporous silica	Synthetic	2.5–25	Pseudo-second-order	Freundlich	298.1–318.1	4.6	Endothermic	Physical	9	446.4	mg/g [31]
5	Graphene oxide	Synthetic	5–15	Pseudo-second-order	Langmuir	—	—	—	—	7	18.6	mg/g [32]
6	Silica-pillared clays (Si-PILC 25) silica-pillared clays (Si-PILC 50) silica-pillared clays (Si-PILC 75)	Natural	18–500	Pseudo-second-order	Sips	—	—	—	—	5	74.5, 61.9, 74.1	mg/g [33]
7	Rice husk char	Synthetic	150–500	—	—	—	—	—	—	—	≥83	% [34]
8	Diatomaceous earth	Natural	20	Pseudo-second-order	Langmuir	—	—	—	—	2	97	% [35]
9	Novel biomaterials from banyan aerial roots	Synthetic	60	Pseudo-second-order	Freundlich	—	—	—	—	8	103.4	% [36]
10	Coal fly ash, kaolinite, perlite, talc, vermiculite	Natural and synthetic	25–100	Pseudo-second-order	Freundlich	—	—	—	—	—	3, 3, 4.5, 3, 3	3.1, 500, 0.8, 6.0, 11.9 mg/g [37]

11	Ethylene diaminetetraacetic acid- β -cyclodextrin	Synthetic	100	Pseudo-second-order	Dubinin-Radushkevich	298.1-318.1	-4.7	Exothermic	Physical	0.209	4-5	448	mg/g	[38]	
12	Groundnut (<i>Ara-chis hypogaea</i>) shell powder and ZnO nanoparticles	Synthetic	10-100	Pseudo-first-order	Freundlich	-	-	-	-	-	6 and 4	79.6 and 85.4	%	[39]	
13	Magnetic fullerene nanocomposite obtained from sustainable PET bottle wastes	Synthetic	500	Pseudo-second-order	Freundlich	303-313	-1.7	Exothermic	Physical	-	6	356-373	mg/g	[40]	
14	Activated carbon montmorillonite, modified montmorillonite, alumina	Natural and synthetic	4	-	-	-	-	-	-	-	-	1.8, 0.6, 1.6,	mg/g	[41]	
15	Derived granular hydrogel with 3D structure	Synthetic	10-600	Pseudo-second-order	Freundlich	-	-	-	-	-	3	267.7	mg/g	[42]	
16	MIL-101(Cr)-HSO ₃	Synthetic	120	Pseudo-second-order	Redlich-Peterson	-	-	-	-	-	8	564.9	mg/g	[43]	
17	Pure SiO ₂ nanoparticle from rice husk	Synthetic	10-120	Pseudo-second-order	Pseudo-second-order	Langmuir	303-323	-33.8	Exothermic	Physical	-	8.5	25.4	mg/g	[44]
18	Guava leaves powder	Synthetic	20-40	Pseudo-second-order	Pseudo-second-order	Langmuir	295-320	9.94	Endothermic	Physical	27.2	4	232.5	mg/g	[45]
19	Hallloysite nanotubes	Synthetic	50	Pseudo-second-order	Freundlich	-	-	-	-	-	6	25.0	mg/g	[46]	
20	Cu@TiO ₂ hybrids consisting of Cu nanoparticles and mesoporous TiO ₂ nanoaggregates	Synthetic	10-160	Pseudo-second-order	Langmuir	-	-	-	-	-	-	888.5	mg/g	[47]	
21	Argentinian montmorillonite	Natural	55-110	Pseudo-second-order	Langmuir	-	-	-	-	-	6	271.7-377.5	mg/g	[48]	
22	Poly(acrylamide-co-itaconic acid)	Synthetic	10-30	Pseudo-second-order	Langmuir	-	-	-	-	-	6	178.5	mg/g	[49]	
23	Kandira stone	Natural	10-40	Pseudo-second-order	Freundlich	293-323	-7.6	Exothermic	Chemical	-	1-1.5	63.9-68.5	%	[50]	
24	Wheat bran	Natural	6.6-29.8	Pseudo-second-order	Dubinin-Radushkevich	298-318	0.0095	Endothermic	Physical	1.1	1.5	159	mg/g	[51]	

(Continued)

Table 1 Continued

No.	Adsorbent	Adsorbent type (natural or synthetic)	Initial Concentration (mg/L)	Fitted model	T (°K)	ΔH° (kJ/mol)	Type of process	E_a (kJ/mol)	Optimum pH	Absorption capacity/ removal efficiency	Unit	References	
25	Pillared clays	Natural	18–500	Sips	—	—	—	—	10	100.6–122.1	mg/g	[52]	
26	Magnetic biosorbents with specific morphological and molecular structure	Synthetic	100–300	Pseudo-second-order	Langmuir 318.1	-10.6	Exothermic	Physical and chemical	5–6.5	527.9	mg/g	[53]	
27	Nickel oxide nanoparticles	Synthetic	50–200	Pseudo-second-order	Freundlich	—	—	—	3	99.8	mg/g	[54]	
28	Regenerated-reed/reed-charcoal	Synthetic	20–50	Hill	Brouers-Sotolongo 323.1	46.0	Endothermic	Physical	—	10.4	76.6	% [55]	
29	Fe ₃ O ₄ coated polymer clay composite	Synthetic	0.5–40	Pseudo-second-order	Freundlich	—	—	—	6–7	39.1	mg/g	[56]	
30	New hybrid supramolecular ionic liquid gels	Synthetic	33.1–331.3	—	—	—	—	—	7	51	%	[57]	
31	Montmorillonite	Natural	500–4,000	—	Langmuir	—	—	—	9	330	mg/g	[58]	
32	Magnesium oxide, chitosan and graphene oxide	Synthetic	30–1,500	Pseudo-second-order	Langmuir	—	—	—	7	1,111	mg/g	[59]	
33	Rice straw biochars prepared under three pyrolytic temperatures	Synthetic	5–60	Pseudo-second-order	Freundlich	—	—	—	8	48.8–131.5	mg/g	[60]	
34	Graphene oxide nanosheets	Synthetic	10–500	Pseudo-second-order and Elovich	Hill and Toth 298	-17.0	Exothermic	Chemical	—	~6–7	>173.4	mg/g	[61]
35	Clickable azido periodic mesoporous organosilicas	Synthetic	0.1	—	—	—	—	—	—	—	0.241	mg/g	[62]
36	Fe-MCM-41s	Synthetic	20–80	Pseudo-second-order and intraparticle diffusion	Freundlich 293–313	9.9	Endothermic	Chemical	—	10	83.3	mg/g	[63]
37	Multi-walled carbon nanotubes	Synthetic	1,000–10,000	—	—	—	—	—	—	—	40–97	%	[64]

38	Activated carbon fiber under electrochemical assistance	Synthetic	50	—	—	—	—	—	—	—	7.4	98.9–99.9 %	[65]
39	Metal-organic frameworks	Synthetic	30–100	Pseudo-second-order	Langmuir	293–323	58.9	Endothermic	Chemical	—	6.8	99.2 %	[66]
40	Chitosan/biochar hydrogel beads	Synthetic	5–160	Pseudo-second-order	Langmuir	—	—	—	—	—	3–10	>76 mg/g	[67]
41	Layered chalcogenides or $K_{2x}Mn_xSn_{3-x}S_6$ ($x = 0.5–0.95$)	Synthetic	10–250	Pseudo-second-order	Langmuir	283–313	11.8	Endothermic	Chemical	—	4–6	199.6–269.5 mg/g	[68]
42	Magnetic nanosorbents with siliceous hybrid shells of alginic acid and carrageenan	Synthetic	50–1,200	Pseudo-second-order	Dubinin–Radushkevich	—	—	—	—	—	2	423–1350 mg/g	[69]
43	Magnetite imprinted chitosan nanocomposite	Synthetic	1–50	Pseudo-second-order	Freundlich	293–338	23.2	Endothermic	Chemical	—	6.5	142 mg/g	[70]
44	Cu(II) and Al(III)-chelated cryogels of N-(2-carboxyethyl) chitosan	Synthetic	3.3–165.6	—	Langmuir	—	—	—	—	—	7–10	280–390 mg/g	[71]
45	Halloysite nanotubes	Synthetic	3.3–397.6	—	Langmuir	298–338	–25.3	Exothermic	Physical	—	5–9	21.6 mg/g	[72]
46	Diesel exhaust emission soot	Synthetic	60	—	—	—	—	—	—	—	7	89 %	[73]
47	Municipal solid waste derived biochar	Synthetic	10–250	Pseudo-second-order and Elovich	Hill	—	—	—	—	—	7–8	190 mg/g	[74]
48	Graphene oxide template-confined fabrication of hierarchical porous carbons derived from lignin	Synthetic	100–280	Pseudo-second-order	Langmuir	298–318	8.5	Endothermic	Physical	—	7	980.4 mg/g	[75]
49	Oil shale powders	Synthetic	0–150	Pseudo-second-order	Langmuir	—	—	—	—	—	3	18.2–43.4 mg/g	[76]
50	As-synthesized single-walled, double-walled and multi-walled carbon nanotubes	Synthetic	5–100	—	Brouers–Sotolongo	—	—	—	—	—	3–7	724 mg/g	[77]

(Continued)

Table 1 Continued

No.	Adsorbent	Adsorbent type (natural or synthetic)	Initial Concentration (mg/L)	Fitted model	Thermodynamic			Optimum pH	Adsorption capacity/ removal efficiency	Unit	References
					Isotherms	T (°K)	ΔH° (kJ/mol)	Endothermic or exothermic process	E_a (kJ/mol)		
51	Diethylenetri-aminopentaacetic acid-functionalized magnetic graphene oxide	Synthetic	0–20	Pseudo-second-order	Freundlich	–	–	–	–	8	70–240 mg/g [78]
52	Porous carrageenan-derived carbons	Synthetic	50	Pseudo-first-order and pseudo-second-order	Langmuir	–	–	–	–	5–8.7	422–459 mg/g [79]
53	Preparation of a specific bamboo based activated carbon	Synthetic	8.42–842	Pseudo-second-order	Langmuir	–	–	–	–	1.5–12.5	613 mg/g [80]
54	CoFe ₂ O ₄ /activated carbon@chitosan	Synthetic	10–30	Pseudo-second-order	Langmuir	–	–	–	–	5	93.5 % [25]
55	Multi-functional activated carbon derived from recycled long-root <i>Eichhornia crassipes</i>	Synthetic	5–15	Pseudo-second-order	Langmuir	283.1–303.1	21.8	Endothermic	Chemical	4	145 mg/g [81]
56	Rabbit manure biochar	Synthetic	5–35	Pseudo-second-order	Langmuir	298–318	6.0–32.6	Endothermic	Physical	–	5 17.7–70.1 mg/g [82]
57	Graphene oxide	Synthetic	1–200	Elovich	Freundlich	–	–	–	–	9	379 mg/g [83]
58	Municipal solid waste biochar – montmorillonite composite	Natural and synthetic	10–250	Pseudo-second-order and Elovich	Hill	–	–	–	–	5	167.3 mg/g [84]
59	Magnetic resin with humic acid	Synthetic	0–66.2	–	–	–	–	–	–	6.5–7	86 % [85]
60	Graphene oxide and reduced graphene oxide polysulfone nanocomposite pellets	Synthetic	13–130	Pseudo-second-order	Freundlich	–	–	–	–	5	21.4–82.7 mg/g [86]
61	Zero-valent iron	Synthetic	21.5	–	–	–	–	–	–	2.5	80 % [87]

62	ZIF-67 derived hollow cobalt sulfide	Synthetic	5–100	Pseudo-second-order	Langmuir	—	—	—	—	—	7	471.7	mg/g [88]
63	Zeolitic imidazolate framework-8 derived nanoporous carbon	Synthetic	5–100	Pseudo-second-order	Freundlich	—	—	—	—	—	6	416.7	mg/g [89]
64	Zeolites prepared from coal fly ash	Synthetic	150	—	—	—	—	—	—	—	3	27.94	% [90]
65	Porous graphene hydrogel	Synthetic	5–100	Boyd	Langmuir	—	—	—	—	—	8	235.6	mg/g [91]
66	Graphene nanosheet	Synthetic	0–300	Elovich	Sips and Hill	—	—	—	—	—	6	113.3–148	mg/g [92]
67	Graphene–soy protein aerogel	Synthetic	1–50	—	Langmuir	—	—	—	—	—	—	500	mg/g [93]
68	Modified coal fly ash	Synthetic	40–140	Pseudo-second-order and intraparticle diffusion	Langmuir	303–323	14.8–28.5	Endothermic	Chemical	—	—	1.5	mg/g [94]
69	Reduced graphene oxide/magnetic composites	Synthetic	5	Pseudo-second-order	Langmuir and Temkin	288–308	−12.2	Exothermic	Chemical	—	6.5	18.2	mg/g [95]
70	Yeast particles via atom transfer radical emulsion polymerization	Synthetic	5–200	Pseudo-second-order	Langmuir and Freundlich	—	—	—	—	—	—	18.4	mg/g [96]
71	Highly porous BN nanosheets	Synthetic	120	Pseudo-second-order	Langmuir	—	—	—	—	—	10	80	% [97]
72	CuO nanoparticles	Synthetic	10–200	—	Freundlich	—	—	—	—	—	7	77	% [98]
73	Graphitic ordered mesoporous carbons	Synthetic	100–200	Pseudo-second-order	Langmuir	298–318	21.7	Endothermic	Chemical	—	6	187–236	mg/g [99]
74	Biochar obtained from used tea leaves	Synthetic	100–500	Pseudo-second-order	Langmuir	—	—	—	—	—	6	238.1	mg/g [100]
75	Zero valent copper nanoparticles	Synthetic	10–40	Pseudo-first-order	—	—	—	—	—	—	3.5	100	% [101]
76	Activated carbon prepared from <i>Enteromorpha prolifera</i>	Synthetic	440	—	Langmuir	303–323	0.4–13.4	Endothermic	Physical	—	2–7	233–286	mg/g [102]
	impregnated with H ₃ PO ₄ and sodium benzenesulfonate												

(Continued)

Table 1 Continued

No.	Absorbent	Adsorbent type (natural or synthetic)	Initial Concentration (mg/L)	Kinetics	Fitted model	Thermodynamic condition	Optimum Adsorption capacity/ removal efficiency	Unit	References	
						ΔH° (kJ/mol)	Type of process	E_a (kJ/mol)	pH	
77	Spray-dried chitosan-metal micro-particles	Synthetic	25–400	Pseudo-second-order	–	–	–	–	0.005–0.3 mg/g	[103]
78	Montmorillonite and kaolinite	Natural	66.2–530.1	–	Langmuir	–	–	–	8 0.52	mg/g [104]
79	UV-accelerated aging of polystyrene and polyvinylchloride	Synthetic	2–25	Pseudo-first-order and pseudo-second-order	Langmuir and Freundlich	–	–	–	6–8.5 0.5–7	mg/g [105]
80	Powder activated carbon and electrospun carbon nanofibers	Synthetic	0.5–20	Pseudo-second-order	Langmuir	–	–	–	6 0.26±0.02 and 0.68±0.04	mg/g [106]
81	Self-regenerating photocatalytic hydrogel	Synthetic	5–100	–	–	–	–	–	5–70 mg/g	[107]
82	Graphene hydrogel	Synthetic	2	–	Langmuir	–	–	–	–	mg/g [108]
83	Molecularly imprinted polymers	Synthetic	0–60	Pseudo-second-order	Langmuir	–	–	–	312 92 %	% [109]
84	Waste sludge	Synthetic	10–80	Pseudo-second-order	–	–	–	–	–	% [110]
85	Birnessite	Natural	0–800	Pseudo-second-order	Langmuir and Freundlich	–	–	–	85	%
86	Activated carbon derived from the residue of desilicated rice husk	Synthetic	150–350	Pseudo-second-order	Langmuir and Koble-Corrigan	298–318	30.7	Endothermic Physical	– 7.9	454.6 mg/g [111]
87	Graphene hydrogel	Synthetic	–	Pseudo-second-order	–	–	–	–	–	189.2–290.5 mg/g [112]
88	Ionic surfactant modified carbon nanotubes	Synthetic	20	Freundlich	–	–	–	–	82–88 %	% [113]
89	Long TiO ₂ nanotubes	–	5–50	Pseudo-second-order	Langmuir	–	–	–	–	5.3–26.3 mg/g [114]

90	Humic acid and levulinic acid coated magnetic Fe_3O_4 nanoparticles	Synthetic	5–30	Pseudo-second-order	Langmuir	–	–	–	–	8	53.7 and 101.9	mg/g [115]	
91	<i>Calotropis gigantea</i> fiber	Synthetic	0–140	Pseudo-second-order	Freundlich	–	–	–	–	8	136.4	mg/g [116]	
92	Wheat straw supported nanoscale zero-valent iron particles	Synthetic	20–100	Pseudo-second-order	Freundlich	–	–	–	–	363.6	mg/g [117]		
93	$\text{V}_2\text{O}_5/\text{ZnO}$ coated carbon nanofibers	Synthetic	10–200	Pseudo-second-order	Langmuir	–	–	–	–	6	87.7	mg/g [118]	
94	Magnetic MIL-101 (Cr)	Synthetic	5–40	Pseudo-second-order	Langmuir	–	–	–	–	8	22.9–63.2	mg/g [119]	
95	KGM/ZIF-8 aerogels were synthesized by combining konjac glucomannan	Synthetic	100–500	Pseudo-second-order	Langmuir	313–323	9.9	Endothermic	Physical	–	7	811.0	mg/g [120]
96	C@silica core/shell nanoparticles from ZIF-8	Synthetic	10–100	–	Freundlich	–	–	–	–	6	1575	mg/g [121]	
97	Graphitic ordered mesoporous carbon	Synthetic	50–200	Pseudo-second-order	Langmuir	–	–	–	–	6	116.7–267.4	mg/g [122]	
98	Organo-vermiculite based on phosphatidylcholine	Synthetic	0–140	Pseudo-second-order	Langmuir	–	–	–	–	8	36.8–93.7	mg/g [123]	
99	Chitosan/kaolin/ Fe_3O_4 magnetic microspheres	Synthetic	20–240	Pseudo-second-order	Langmuir	–	–	–	–	6	47.8	mg/g [124]	
100	Porous covalent organic gels	Synthetic	5–50	Pseudo-second-order	Langmuir	–	–	–	–	10	93.4	% [125]	
101	<i>Calotropis gigantea</i> fiber	Synthetic	50–200	Pseudo-second-order	Langmuir and Freundlich	–	–	–	–	10	64.9–77.3	mg/g [126]	
102	Activated carbon from <i>Enteromorpha prolifera</i>	Synthetic	50–500	Pseudo-second-order	Langmuir	–	–	–	–	7–9	216.5	mg/g [127]	
103	Activated carbon from waste <i>Salix psammophila</i>	Synthetic	0–200	Pseudo-second-order	Langmuir and Freundlich	–	–	–	–	7.5	366.9	mg/g [128]	

(Continued)

Table 1 Continued

No.	Adsorbent	Adsorbent type (natural or synthetic)	Initial Concentration (mg/L)	Fitted model		Thermodynamic				Optimum pH	Adsorption capacity/ removal efficiency	Unit	References	
				Kinetics	Isotherms	T (°K)	ΔH° (kJ/mol)	Type of process	E_a (kJ/mol)					
104	Novel semi-fluid Fe/ charcoal micro-electrolysis reactor	Synthetic	10–35	—	—	—	—	—	—	5.3	54.5–95.5	%	[129]	
105	One-pot self-assembly of 3D CdS-graphene aerogels	Synthetic	20	—	—	—	—	—	—	85.8	%	%	[130]	
106	Novel Fe_3O_4 / Graphene oxide/citrus peel-derived biochar	Synthetic	10–160	Pseudo-second-order	Freundlich	—	—	—	—	6	283.4	mg/g	[131]	
107	Novel chalcogenide based magnetic adsorbent KMnS-1/L-Cystein/ Fe_3O_4	Synthetic	10–200	Pseudo-second-order	Langmuir	—	—	—	—	6	181.3	mg/g	[132]	
108	Novel alginate particles decorated with nickel	Synthetic	20–120	Pseudo-second-order	Langmuir	—	—	—	—	7	135.1	mg/g	[133]	
109	Nanostructured diatomite	Synthetic	20–40	—	—	—	—	—	—	6	18–75	%	[134]	
110	Microporous activated carbon	Synthetic	20–100	Pseudo-second-order	Langmuir	303–323	20.5	Endothermic	Physical	9	96.1	%	[135]	
111	(MoS_4^2-) ²⁻ -intercalated CaMoS_4 :LDH material	Synthetic	50	Pseudo-second-order	Langmuir	—	—	—	—	6	707.2	mg/g	[136]	
112	Montmorillonite	Natural	40	—	—	—	—	—	—	7	23	mg/g	[137]	
113	Magnetic carbon composite, $\text{Fe}_3\text{O}_4/\text{C}$ composite	Synthetic	10–60	Pseudo-second-order	Langmuir	293–313	13.3	Endothermic	Physical	—	8	90.1	mg/g	[138]
114	MIL-53 (Fe)-directed synthesis of hierarchically mesoporous carbon	Synthetic	10	Pseudo-second-order	Langmuir	—	—	—	—	4	90.9	mg/g	[139]	
115	Kaolinite	Natural	33.1–662.6	Pseudo-second-order	Langmuir	—	—	—	—	—	5–9	4.9	mg/g	[140]

116	Nanosized magnetite	Synthetic	0.33–165.6	—	Freundlich	—	—	—	6	45–80	% [141]
117	Magnetic mesoporous carbon material	Synthetic	400–800	Pseudo-second-order	Langmuir	288–318	65.5	Endothermic	—	6.8	868.6 mg/g [142]
118	Magnetic copper-based metal-organic framework	Synthetic	10–80	Pseudo-second-order	Langmuir	298–318	48.6	Endothermic	Physical	—	538 mg/g [143]
119	Magnetic Co-based carbon materials derived from core-shell metal–organic frameworks	Synthetic	16.56	—	—	—	—	—	3–10	88.5	% [144]
120	Magnetic biochar-based manganese oxide composite	Synthetic	2–16	Pseudo-second-order	Langmuir	288–308	16.6	Endothermic	Physical	—	3–4 mg/g [145]
121	Magnetic alginate-Fe ₃ O ₄ hydrogel fiber	Synthetic	10	—	—	—	—	—	3	0.42–12.2	mg/g [146]
122	Low-cost magnetic herbal biochar	Synthetic	5–300	Pseudo-second-order	Langmuir	—	—	—	6	68.9 ± 3.2	mg/g [147]
123	Low-cost biochar derived from herbal residue	Synthetic	10–300	Pseudo-second-order	Freundlich	—	—	—	7	37.6 ± 0.87	mg/g [148]
124	Red mud	Natural	10–100	Pseudo-second-order	Freundlich	—	—	—	—	96.5	% [149]
125	Palygorskite montmorillonite filter medium	Synthetic	1,500	Pseudo-second-order and Elovich	Langmuir	—	—	—	—	100–111	mg/g [150]
126	Graphene oxide (GO) reinforcement on keratin based smart hydrogel	Synthetic	1–950	Elovich	Langmuir and Sips	—	—	—	5	28 ± 3–55	mg/g [151] ± 6
127	Laponite crosslinked sodium alginate/k-carrageenan double-network gel beads	Synthetic	20–300	Pseudo-second-order	Langmuir and Freundlich	293.1–303.1	-2.6–0.5	Exothermic	Physical and chemical	5	245.1 mg/g [152]
128	Titanium dioxide nanoparticles	Synthetic	0.02–0.5	—	Freundlich	—	—	—	—	53.6 ± 7.2	% [153]

(Continued)

Table 1 Continued

No.	Adsorbent	Adsorbent type (natural or synthetic)	Initial Concentration (mg/L)	Fitted model	Thermodynamic			Optimum pH	Absorption capacity/ removal efficiency	Unit	References
					Kinetics	Isotherms	T (K)	ΔH° (kJ/mol)	Endothermic or exothermic condition		
										E _a (kJ/mol)	
129	Porous resins	Synthetic	20–100	Pseudo-second-order	Langmuir	—	—	—	—	7	25–130 mg/g [154]
130	Stabilized Fe-Mn binary oxide nanoparticles	Synthetic	5–100	Pseudo-second-order	Langmuir	—	—	—	—	6	1172.2 mg/g [155]
131	Cationic and anionic flax noil cellulose	Synthetic	80	Pseudo-second-order and intraparticle diffusion	Langmuir	303.1	−17.1 and 9.9	Exothermic and endothermic	Physical	11.10 and 7.87	6.5 156.9–238.7 mg/g [156]
132	Palygorskite montmorillonite	Natural	100–1,500	—	Langmuir	298–348	11.4	Endothermic	Physical	—	5 0.077–107 mg/g [157]
133	Synthesized bimessite	Synthetic	500–6,000	Pseudo-second-order	Langmuir	—	—	—	—	9	419–442 mg/g [158]
134	Activated carbon, bentonite, zeolite, and pumice	Synthetic	20–40	Pseudo-second-order	—	295	6–8.6	Endothermic	Physical	—	91.87, 51, and 25 % [159]
135	<i>Corylus avellana</i> (hazelnut) activated carbon	Synthetic	25–200	Pseudo-second-order	Langmuir	273–323	3.06	Endothermic	Physical	—	6 61.2–73.6 mg/g [160]
136	Ordered mesoporous carbon and bamboo-based carbon	Synthetic	20–100	Pseudo-second-order	Langmuir	298–318	18.4–35.4	Endothermic	Physical	—	6 233.3 and 362.9 mg/g [161]
137	Activated carbon powder	Synthetic	20–1,200	Pseudo-second-order	Langmuir	—	—	—	—	8	434.7 mg/g [7]
138	ZnO nanoparticles and groundnut shell	Synthetic	80–100	—	Thomas and Yoon-Nelson	—	—	—	—	4–6	5.0–6.1 and 5.8–6.7 mg/g [162]
139	Porous hydrogen-bonding covalent organic polymers	Synthetic	2–20	Pseudo-second-order	Langmuir	—	—	—	—	6	6.1–8.4 mg/g [163]
140	Facile hydrothermal synthesis of magnetic adsorbent CoFe ₂ O ₄ /MMT	Synthetic	50–120	Pseudo-second-order	Langmuir	298–318	−25.3	Exothermic	Chemical	—	6 224 mg/g [164]

141	Raphene-soy protein biocomposites	Synthetic	10–50	—	Langmuir and Temkin	—	—	—	4	500	mg/g	[165]			
142	Biocomposite fibers of graphene oxide/calcium alginate	Synthetic	5–70	Pseudo-second-order	Langmuir	—	—	—	6.5	18.45–39.06	mg/g	[166]			
143	Montmorillonite impregnated cellulose acetate nanofiber membrane	Synthetic	10	—	—	—	—	—	4	27–>90	%	[167]			
144	Magnetic polyani-line/graphene oxide based nanocomposites	Synthetic	10–150	Pseudo-second-order	Freundlich	298–318	63.8	Endothermic	Chemical	—	—	—			
145	Pretreated oat hulls	Synthetic	4.8–60	Pseudo-second-order	Freundlich	298–318	17	Endothermic	Physical	—	1	83	mg/g	[169]	
146	Humic acid modified hydrogel beads	Synthetic	20–250	Pseudo-second-order	Langmuir	—	—	—	—	—	8	61.2	mg/g	[170]	
147	Sludge-derived biochar	Synthetic	0–50	—	—	—	—	—	—	—	6	41.6–47.8	%	[171]	
148	Activated graphene	Synthetic	40–200	Pseudo-second-order	Langmuir	—	—	—	—	—	8	~194.6	mg/g	[172]	
149	Modified alginate/graphene double network porous hydrogel	Synthetic	50–500	Pseudo-second-order	Langmuir	—	—	—	—	—	2	247.5–290.7	mg/g	[173]	
150	Polypyrrole functionalized <i>Calotropis gigantea</i> fiber	Synthetic	0–200	Pseudo-second-order	Langmuir	—	—	—	—	—	6	78.2	mg/g	[174]	
151	Potassium hydroxide (KOH) modified biochar derived from potato stems and leaves	Synthetic	2–16	Pseudo-second-order	Langmuir	288.1–308.1	14.2 and 23.4	Endothermic	Physical	—	9	23.3	mg/g	[175]	
152	Regenerable long TiO ₂ nanotube/graphene oxide hydrogel	Synthetic	1–200	—	Langmuir	—	—	—	—	—	—	—	108.7–178.6	mg/g	[176]
153	Surface functionalized superparamagnetic porous silicas	Synthetic	0.01–0.3	Pseudo-second-order	Freundlich	—	—	—	—	—	5	5–108	mg/g	[177]	

Table 1 Continued

No.	Adsorbent	Adsorbent type (natural or synthetic)	Initial Concentration (mg/L)	Kinetics	Isotherms	T (°K)	ΔH° (kJ/mol)	Type of process	E_a (kJ/mol)	Thermodynamic		Optimum pH	Adsorption capacity/ removal efficiency	Unit	References	
										Fitted model	Condition					
154	Ag/AgCl@N-doped activated carbon composite	Synthetic	100	Pseudo-first-order	—	—	—	—	—	—	—	—	47.5–62.5	%	[178]	
155	Magnetic activated carbon/chitosan nanocomposite	Synthetic	5–60	Pseudo-second-order	Langmuir	—	—	—	—	—	—	—	90.1	mg/g	[179]	
156	Simultaneous activated and magnetic ZnO-doped biochar derived from camphor leaves	Synthetic	30–300	Pseudo-second-order	Langmuir	—	—	—	—	—	—	4	449.4	mg/g	[180]	
157	Fixed-bed column, packed with SG-C650H resin	Synthetic	100–200	—	Langmuir	—	—	—	—	—	—	—	81.5	%	[181]	
158	Bamboo charcoal	Synthetic	0.5–70	Pseudo-second-order	Langmuir	—	—	—	—	—	—	—	5.5	36.0 ± 1.9	mg/g	[182]
159	Magnetic metal-organic framework sorbents	Synthetic	50–250	Elovich and Pseudo-second-order	Langmuir	298–328	18.3	Endothermic	Physical	—	—	6	322.5	mg/g	[183]	
160	Metal-organic framework	Synthetic	5–250	Pseudo-second-order	Langmuir	—	—	—	—	—	—	6	88.9	mg/g	[184]	
161	Magnetic multifunctional resin the presence and absence of humic acid	Synthetic	20	Freundlich and Langmuir	—	—	—	—	—	—	—	10	15–53	%	[185]	
162	Carbon nanofibers	Synthetic	0.5–3	Pseudo-second-order	Langmuir	—	—	—	—	—	—	6	10.3	mg/g	[186]	
163	Modified waste grapefruit peel	Synthetic	56.1–1,656.7	Pseudo-second-order	Langmuir	—	—	—	—	—	—	7	96.4	%	[187]	
164	Fly ash, activated carbon, bentonite and bagasse ash	Natural and synthetic	31.3–66.2	Pseudo-second-order	Temkin	—	—	—	—	—	—	—	78.4–90.8, 86.2–92, 88.7–93.2, and 88.2–91.3	%	[188]	

165	Magnetic graphene oxide/nitrilotriacetic acid nanocomposite	Synthetic	10–100	Pseudo-second- order	Freundlich	283–313	3.6	Endothermic	Physical	–	10	263.7–334.7 mg/g	[189]
166	Nanostructured chitin/graphene oxide hybrid material	Synthetic	0–700	Pseudo-second- order	Sips	–	–	–	–	–	9	70–300 mg/g	[190]
167	Rice husk biochars	Synthetic	5–60	Pseudo-second- order	Langmuir	–	–	–	–	–	9	36.1 mg/g	[191]
168	Dry-mixing and wet-mixing activated carbons prepared from waste printed circuit boards by NaOH activation	Synthetic	20–800	Pseudo-second- order	Langmuir	298–318	8.1–13.2	Endothermic	Physical	–	8	381.2–603.8 mg/g	[192]
169	Coating magnetic biochar with humic acid	Synthetic	2–18	Pseudo-second- order	Langmuir	288–388	5.5	Endothermic	Physical and chemical	–	10	11.4 mg/g	[193]
170	Titanate nanotubes	Synthetic	3.3–165.6	Pseudo-second- order	Langmuir	–	–	–	–	–	4	18.9 mg/g	[194]
171	Functionalized ferromagnetic 3D NiFe ₂ O ₄ porous hollow microsphere	Synthetic	0–10	Pseudo-second- order	Freundlich	–	–	–	–	–	5	>80 %	[195]
172	Different micro-structured tourmaline, halloysite and biotite	Synthetic	0–50	Pseudo-second- order	Redlich-Peterson	–	–	–	–	–	6	21.7 mg/g	[196]
173	Graphene and granular activated carbon	Synthetic	2–60	Pseudo-second- order	Langmuir	298–338	–5.8	Exothermic	Physical	–	4–6	323 mg/g	[197]
174	Chemically prepared carbon from date palm leaflets	Synthetic	50–300	Pseudo-second- order	Langmuir	298–318	11.6–13.1	Endothermic	Physical	17	6	104.2–133.3 mg/g	[198]
175	Activated carbons prepared from biomass wastes by H ₃ PO ₄ activation	Synthetic	100–800	Pseudo-second- order	Langmuir	–	–	–	–	–	8.5–12.5	244–400 mg/g	[199]
176	Candle soot coated polyurethane foam	Synthetic	60	Pseudo-second- order	Langmuir	–	–	–	–	–	2	80 %	[200]
177	Clinoptilolite	Natural	2–10	Pseudo-second- order	Langmuir	298–338	–29.9	Exothermic	Physical	–	6	5.4 mg/g	[201]

(Continued)

Table 1 Continued

No.	Adsorbent	Adsorbent type (natural or synthetic)	Initial Concentration (mg/L)	Kinetics	Fitted model	Thermodynamic			Optimum pH	Adsorption capacity/ removal efficiency	Unit	References
						T (°K)	ΔH° (kJ/mol)	Type of process				
178	<i>Enteromorpha prolifera</i>	Natural	12.5–125	Pseudo-second-order	Freundlich	–	–	–	–	10	21.7	mg/g [202]
179	Kaolinitic clay and hematite	Natural	6.6–66.2	Pseudo-second-order	Temkin	303–343	–8.4 and –9.9	Exothermic	Physical	–	5–9	0.53 and 0.02 mg/g [203]
180	Amine-functionalized magnetic bamboo-based activated carbon	Synthetic	300	–	Langmuir	–	–	–	–	6	131.6–245.6	mg/g [204]
181	Boron nitride nanomaterials	Synthetic	10–100	Pseudo-second-order	Langmuir	–	–	–	–	4–6	1.3–1.6	mg/g [205]
182	Pectin-functionalized magnetic nanoparticles	Synthetic	5–10	Pseudo-second-order	Sips	–	–	–	–	7	89	% [206]
183	Sodium alginate/graphene oxide composite beads	Synthetic	10–150	Pseudo-second-order	Langmuir	–	–	–	–	4	4.2–86.1	mg/g [207]
184	Poly(methacrylic acid) hydrogels	Synthetic	10–50	–	Langmuir	289–310	170.2	Endothermic	Chemical	–	5–8	10 mg/g [208]
185	Nano-hydroxyapatite	Synthetic	0–25	Pseudo-second-order	Langmuir and Freundlich	–	–	–	–	6	47.3	% [209]
186	Multi-walled carbon nanotubes with different oxygen contents	Synthetic	10–160	Intraparticle diffusion and outer diffusion	Dubinin–Radushkevich and Langmuir	–	–	–	–	4	150.6–206	mg/g [210]
187	Activated carbon prepared from lignin with H_3PO_4 activation	Synthetic	180–600	Pseudo-second-order	Langmuir	293–313	–4.1	Exothermic	Chemical	–	–	418.6 mg/g [211]
188	Nanoscale zerovalent iron with copper bimetallic particles	Synthetic	50–200	Pseudo-first-order	–	–	–	–	–	6	81.6–92.9	% [212]
189	Polyvinylpyrrolidone stabilized NZVI/Cu bimetallic particles	Synthetic	50–200	Pseudo-first-order	–	–	–	–	–	6	95.6	% [213]

190	Titanium-based tri-metal oxide mesh type anode, activated charcoal	Synthetic	20	Pseudo-second-order	-	-	-	5.4	93.6–99.1	%	[214]	
191	Hierarchical CuS hollow nano-spheres@N-doped cellulose nanocrystals hybrid composites	Synthetic	20	Pseudo-first-order	-	-	-	-	43.5–66	%	[215]	
192	Hydrophilic and strengthened 3D reduced graphene oxide/nano- Fe_3O_4 hybrid hydrogel	Synthetic	0.5–50	Pseudo-second-order	-	-	-	5–8	86	%	[216]	
193	Carbon nanosheets supported TiO_2	Synthetic	5–40	Pseudo-second-order	Freundlich	-	-	7	40.5	mg/g	[217]	
194	Nano-zinc oxide incorporated graphene oxide/nanocellulose composite	Synthetic	2–4	Pseudo-first-order	Sips	-	-	5.5	98	%	[218]	
195	Sodium alginate/graphene oxide hydrogel beads	Synthetic	20–80	Pseudo-second-order	Freundlich	-	-	7	100	mg/g	[219]	
196	Diesel soot coated non-woven fabric	Synthetic	25	-	-	-	-	-	97	%	[220]	
197	Rice husk	Natural	0.000005–0.001	-	-	-	-	-	32	mg/g	[221]	
198	Magnetic graphene oxide-grafted cellulose nanocrystal molecularly imprinted polymers	Synthetic	0–1,000	Pseudo-second-order	Freundlich	-	-	6–8	3.7–5.2	mg/g	[222]	
198	ZnO nanoparticles	Synthetic	10–100	-	-	-	-	-	4	15–90	%	[224]

(Continued)

Table 2
Adsorption processes applied with different adsorbents to adsorb ciprofloxacin from wastewater media resulting from papers published from 1990 to 2020 the type and nature of the adsorbent, initial concentration (mg/L), fitted models (kinetics and isotherms), thermodynamic parameters (T (°K), ΔH° (kJ/mol)), optimum pH, optimum capacity (E_a (kJ/mol)), optimum pH, adsorption capacity/ removal efficiency (%) and removal efficiency (%)

No.	Adsorbent	Adsorbent type (natural or synthetic)	Initial concentration	Fitted model		Thermodynamic			Type of process	E_a (kJ/mol)	Optimum pH	Adsorption capacity/ removal efficiency	Unit	References
				Kinetics	Isotherms	T (°K)	ΔH° (kJ/mol)	Endothermic or exothermic condition						
1	Clay soil, quartz sand and solid matter isolated from the piggery wastewater	Natural	0.000002–0.5	—	—	—	—	—	—	—	—	>95	%	[224]
2	Sawdust	Natural	10–20	Pseudo-second-order	—	—	—	—	—	—	5.8	80	%	[225]
3	Combined cross-linked enzyme aggregate	Synthetic	16.5–662.6	—	—	—	—	—	—	—	4.5–5.5	>80	%	[226]
4	Activated carbon produced from Jerivá mud-nanoparticles	Synthetic	100–900	Avrami	Liu	288–318	3.3	Endothermic	Physical	—	7	335.8	mg/g	[227]
5	Magnetic Fe_3O_4 /red mud-nanoparticles	Synthetic	3	Pseudo-second-order	Freundlich	—	—	—	—	—	6.5	110.1	mg/g	[228]
6	One-pot synthesis of trifunctional chitosan-EDTA- β -cyclodextrin polymer	Synthetic	0–66.2	Pseudo-second-order	Sips	—	—	—	—	—	3–8	0.053	mg/g	[229]
7	Activated sludge of the sewage treatment plant	Synthetic	0.5–10	—	—	—	—	—	—	—	—	96	%	[230]
8	Functionalized magnetic nanoparticles	Synthetic	5–20	Pseudo-second-order	Langmuir	—	—	—	—	—	7	85	%	[231]
9	<i>Ficus benjamina</i> wood chip-based aerated biofilter	Synthetic	0.005	—	—	—	—	—	—	—	—	81	%	[232]

10	Aerobic activated sludge system	Synthetic	0.1	Pseudo-first-order	-	-	-	-	95	%	[233]	
11	Laboratory-scale membrane bioreactors	Synthetic	0–0.5	Pseudo-first-order	-	-	-	-	52.8	%	[234]	
12	Anaerobic sulphate-reducing bacteria sludge system	Synthetic	0.1–5	Pseudo-first-order	Henry and Freundlich	278–308 -20–80	Exothermic	Physical and chemical	-	20–90	%	[235]
13	Aerobic and anoxic activated sludge process	Synthetic	0.1–0.3	Pseudo-second-order and order and general-rate-law	Henry and Freundlich	290–303 -29.5	Exothermic	Physical	7.3	939.2–1,517.2 and 461.1–1,844.2	mg/g	[236]
14	Sulfate-reducing bacteria sludge	Synthetic	0.1–5	Pseudo-second-order	Freundlich	-	-	-	7	30 and 90	%	[237]
15	Pomegranate peels	Natural	100–10,000	Pseudo-second-order	Langmuir	-	-	-	4–5	999	mg/g	[238]
16	Activated charcoal entrapped within zinc-pectinate beads	Synthetic	100–500	-	-	-	-	-	>0.45	mg/g	[239]	
17	SiO ₂ nanoparticle	Synthetic	25–100	Pseudo-second-order	Langmuir	-	-	-	174.5	mg/g	[240]	
18	Different carbon materials	Synthetic	100	-	Guggenheim–Anderson–De Boer and Sips	-	-	-	264	mg/g	[241]	
19	<i>Rhodococcus</i> sp. B30 strain	Natural	0.01–0.15	-	Freundlich	-	-	-	5.5	2–30	%	[217]
20	Activated sludge derived granular activated carbon	Synthetic	20–100	Pseudo-second-order	Langmuir	-	-	-	7	14–16	mg/g	[242]

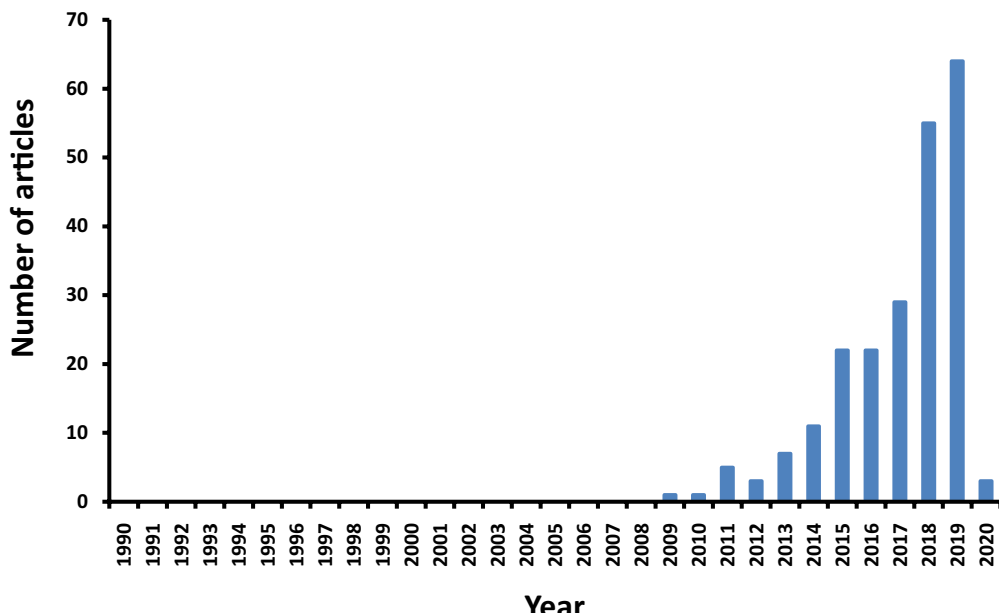


Fig. 3. Number of relevant publications from 1990 to 2020.

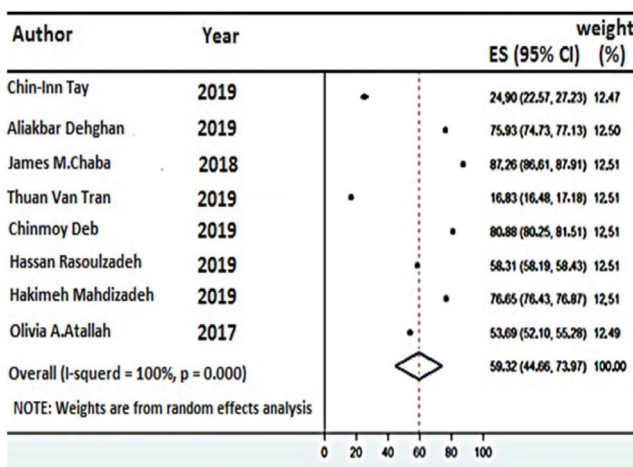


Fig. 4. Forest plot of mean efficiencies of ciprofloxacin removal by the adsorption process.

4.1. Adsorbent type

The type and nature of the adsorbent were considered as the effective factors on the adsorption capacity and removal efficiency of ciprofloxacin [243]. According to Tables 1 and 2, the adsorbents used for the adsorption of ciprofloxacin originated from different natural and synthetic materials. According to Fig. 2b, 22 (10.04%) of adsorbents were natural adsorbents, 4 (1.82%) natural and synthetic, and 193 (88.12%) had a synthetic nature. In the reviewed papers, natural sorbents such as bentonite, diatomaceous earth, montmorillonite, kaolinite, birnessite, clinoptilolite, hematite, silica-pillared clays, sawdust, wheat bran, rice husk, *Enteromorpha prolifera*, clay soil, and etc and synthetic sorbents such as synthesized nanoceria, chitosan grafted $\text{SiO}_2-\text{Fe}_3\text{O}_4$ nanoparticles, zinc oxide supported on Santa Barbara

Amorphous SBA-15 type mesoporous silica, ethylene diaminetetraacetic acid- β -cyclodextrin, groundnut shell powder and zinc oxide (ZnO) nanoparticles, magnetic fullerene nanocomposite obtained from sustainable polyethylene terephthalate bottle wastes, and etc have been used.

By reviewing the adsorbents used to remove ciprofloxacin in various studies, it was observed that a number of adsorbents showed high adsorption capacity, for example, adsorbents containing carbon and graphene, clay adsorbents, magnetic adsorbents, and nanoparticles. In addition, most adsorbents with high adsorption capacity had a synthetic nature.

4.2. Initial concentration of ciprofloxacin

The concentrations of ciprofloxacin in the aqueous media were measured by one of the methods of spectrophotometry or high-performance liquid chromatography. A review of the literature showed that an initial concentration of ciprofloxacin in the range of 2 ng/L to 10,000 mg/L was used. Ciprofloxacin concentrations were reported to be 0.001 mg/L in effluent and surface water, more than 0.15 mg/L in hospital wastewater, and 30 mg/L in pharmaceutical wastewater [11]. It can be concluded that the concentration ranges of ciprofloxacin used in the studies completely covered the concentration of ciprofloxacin in real environments. By reviewing the concentrations used in the studies, we found that in most studies, concentrations ranging from 5 to 500 mg/L demonstrated a high adsorption capacity.

4.3. Optimum pH of the solution

Since pH affects the surface charge of the adsorbent and ciprofloxacin structure, it is considered an important factor for adsorption [243–245]. In 94 articles (42.15%), the optimum pH ranged from 6 to 8.5, which is close to the

Table 3

Experimental conditions of the studies included in the meta-analysis

Type of adsorbent	Initial concentration (mg/L)	Optimum pH (-)	Optimum reaction time (min)	References
Guava leaves	20–40	4	60	Tay and Ong [45]
Metal–organic frameworks	301–100	6.8	39.95	Dehghan et al. [66]
V ₂ O ₅ /ZnO coated carbon nanofibers	10–200	6	20	Chaba and Nomngongo [118]
MIL-53 (Fe)-directed synthesis of hierarchically mesoporous carbon	10	4	120	Tran et al. [139]
Fly ash, activated carbon, bentonite and bagasse ash	31.3–66.2	–	360	Deb et al. [188]
Magnetite imprinted chitosan nanocomposite	1–50	6.5	200	Rasoulzadeh et al. [70]
Semi-fluid Fe/charcoal micro-electrolysis reactor	10–35	5.3	105	Mandizadeh et al. [129]
Pectin-functionalized magnetic nanoparticles	5–10	7	30	Attallah et al. [206]

values recommended by the World Health Organization (WHO), the Environmental Protection Agency (EPA) and the Food and Agriculture Organization (FAO) for discharging effluent for irrigation, which is an advantage for the process because it does not need to adjust the solution pH. In addition, in most studies, the optimum pH was 6.

4.4. Fitted kinetic and isotherm models

Kinetic equations are used to describe the transfer behavior of adsorbed molecules per time and study variables affecting the reaction rate [243]. In addition, models and equations of adsorption equilibrium isotherms are used to describe the adsorbent surface properties, provide insight into the adsorption process, and report experimental data [244]. Isotherms are also considered an important factor in designing adsorption systems and describing the relationship between the adsorbate concentration and adsorption capacity of an adsorbent [245]. It was found that in most articles, the adsorption data fitted well with the Langmuir isotherm and the pseudo-second-order kinetic models (Tables 1 and 2). However, some studies well fitted with Freundlich [28,31], Sips [33,52], Dubinin–Radushkevich [38,51,69], Redlich–Peterson [41,196], Brouers–Sotolongo [55,77], Hill and Toth [61], Temkin [165,203], Koble–Corrigan [111], Thomas and Yoon–Nelson [39], Liu [227], and Guggenheim Anderson and De Boer [241] isothermal models. Also, some studies well fitted with pseudo-first-order [29,39], intraparticle diffusion [63,94,156], Elovich [92,151], Boyd [91], and Avrami [227] kinetics models.

4.5. Thermodynamic model

The concept of thermodynamics hypothesizes that energy cannot be gained or lost and the entropy change is the driving force in an isolated system [243–245]. The results of reviewing the articles showed that a limited number of articles examined thermodynamics. In addition, in articles involving thermodynamics studies, the temperature and standard enthalpy change (ΔH°) varied in the range of 273°K–388°K and -1,212.6–170.21 kJ/mol, respectively (Tables 1 and 2). We found few studies reported activation

energy values ($n = 4$ articles). Although the process of ciprofloxacin adsorption in aqueous medium has been reported both physically and chemically. But in most studies, the process of ciprofloxacin adsorption was physical. A total of 53 papers examined thermodynamic parameters. According to the studies, the adsorption process of ciprofloxacin in aqueous medium was both endothermic ($n = 35$ articles) and exothermic ($n = 17$ articles). In one article, the process of ciprofloxacin adsorption was reported both exothermic and endothermic.

4.6. Adsorption capacity and removal efficiency

According to Tables 1 and 2, many papers reported an adsorption capacity greater than 100 mg/g. In the reviewed studies, the minimum and maximum adsorption capacities were related to birnessite (47 ng/g) [19] and C@silica core/shell nanoparticles from ZIF-8 (1,575 mg/g) [121], respectively.

A number of studies have shown high adsorption capacity, for example; Genç et al. [29] used bentonite adsorbent and initial concentrations of 50–500 mg/L to adsorb ciprofloxacin from water and reported adsorption capacity of 147.06 mg/g. In a study by Danaloğlu et al. [30], chitosan grafted SiO₂–Fe₃O₄ nanoparticles and initial concentrations of 5–40 mg/L were used to remove ciprofloxacin from water showed an adsorption capacity of 100.74 mg/g. Moreover, the adsorption data fitted well with the Langmuir isotherm and the pseudo-second-order kinetic models. Sousa et al. [31] used zinc oxide supported on SBA-15 type mesoporous silica and initial concentrations of 5–40 mg/L to adsorb ciprofloxacin from water and reported an optimum pH of 9 and adsorption capacity of 446.42 mg/g. In addition, the results of researchers have shown that the adsorption data fitted well with the Freundlich isotherm and the pseudo-second-order kinetic models. In thermodynamic studies, they used a temperature of 298.15°K–318.15°K and obtained a ΔH° of 4.67. Yu et al. [38] used ethylene diaminetetraacetic acid–β-cyclodextrin and ciprofloxacin initial concentrations of 100 mg/L to adsorb from water and reported an optimum pH 4–5 and adsorption capacity of 335.8 mg/g. Moreover, the adsorption data fitted well

with the Dubinin–Radushkevich isotherm and the pseudo-second-order kinetic models. In thermodynamic studies, researchers used a temperature of 298.15–318.15°K and obtained a ΔH° of -4.74. De Oliveira Carvalho et al. [227] used activated carbon produced from Jerivá and ciprofloxacin initial concentration of 100 mg/L to adsorb from wastewater. They reported an optimum pH of 7 and adsorption capacity of 335.8 mg/g. Also, the adsorption data fitted well with the Liu isotherm and the Avrami kinetic models. In thermodynamic studies, they used a temperature of 288°K–318°K and showed a ΔH° of 3.34. Aydin et al. [228] used magnetic Fe_3O_4 /red mud-nanoparticles and ciprofloxacin initial concentration of 3 mg/L to adsorb from wastewater and reported an optimum pH 6.5 and adsorption capacity of 110.15 mg/g. In addition, the adsorption data fitted well with the Freundlich isotherm and the pseudo-second-order kinetic models.

In addition, a number of studies reported very low adsorption capacities, for example; Dube et al. [37] used perlite, coal fly ash, talc, and vermiculite as adsorbent and ciprofloxacin initial concentrations of 25–100 mg/L to adsorb from water and reported an optimum pH 3–4.5 and adsorption capacities of 0.81 to 11.93 mg/g. Also, the adsorption data fitted well with the Freundlich isotherm and the pseudo-second-order kinetic models. In a study by Avci et al. [41], in the use of activated carbon, montmorillonite, modified montmorillonite, and alumina as adsorbent and initial concentration of 4 mg/L to the removal of ciprofloxacin from water showed adsorption capacities of 0.6–1.86 mg/g. In research by Gao et al. [62], in the use of clickable azido periodic mesoporous organosilica as adsorbent and initial concentration of 0.1 mg/L to the removal of ciprofloxacin from water showed an adsorption capacity of 0.241 mg/g. Reynaud et al. [103] used spray-dried chitosan-metal microparticles adsorbent and initial concentrations of 25 to 400 mg/L to adsorb ciprofloxacin from water and reported adsorption capacities of 0.005–0.35 mg/g. Also, their results show that the adsorption data fitted well with the pseudo-second-order kinetic model.

A number of studies recorded removal efficiencies above 85%, for example; in a study by Malik et al. [231], functionalized magnetic nanoparticles and ciprofloxacin initial concentrations of 5–20 mg/L were used to remove from wastewater showed an optimum pH of 7 and removal efficiency of 85%. Moreover, the adsorption data fitted well with the Langmuir isotherm and the pseudo-second-order kinetic models. García-Alonso et al. [35] used diatomaceous earth and an initial concentration of 20 mg/L to adsorb ciprofloxacin from water and reported a removal efficiency of 97%. In addition, the results of researchers have shown that the adsorption data fitted well with the Langmuir isotherm and the pseudo-second-order kinetic models. Dhiman and Sharma [39] used ZnO nanoparticles and ciprofloxacin initial concentrations of 10–100 mg/L to adsorb from water and reported an optimum pH 4 and removal efficiency of 85%. Moreover, the adsorption data fitted well with the Freundlich isotherm and the pseudo-first-order kinetic models. Wang et al. [65], used activated carbon fiber in combination with the electrochemical process to remove ciprofloxacin (initial

concentration of 50 mg/L) from water media with an optimal pH of 7.4 and removal efficiencies of 98.9%–99.9%.

4.7. Meta-analysis

As shown in Fig. 4, the results of the meta-analysis revealed a mean ciprofloxacin removal efficiency of 59.32% (95% CI: 44.66–73.97) using the adsorption process.

5. Conclusion, recommendations, and perspectives

The available literature reviewed here has shown a growing interest in recent years in adsorption process application for the removal of ciprofloxacin from aqueous media. Although a wide range of adsorbents has been used to adsorb ciprofloxacin over the past decade, magnesium oxide/chitosan/graphene oxide nanoparticles, magnetic nanosorbents with siliceous hybrid shells of alginic acid and carrageenan and C@silica core/shell nanoparticles from ZIF-8 had shown a better performance (adsorption capacity > 1,000 mg/g). The highest adsorption capacity reported for ciprofloxacin was 1,575 mg/g for C@silica core/shell nanoparticles from ZIF-8. In 94 articles (42.15%), the pH ranged from 6 to 8.5, which is close to the values suggested by the WHO, EPA, and FAO for discharging effluent for irrigation. This review has successfully elucidated the progress in ciprofloxacin removal. It can be concluded that adsorption is an effective technique of mitigating ciprofloxacin pollution in the aqueous media. In addition, regarding the importance of selecting environmentally friendly processes, the use of natural adsorbents and green synthesis methods can be suggested.

Acknowledgments

The authors would like to thank the Environmental Health Engineering Research Center affiliated to Kerman University of Medical Sciences and Cardiogenetic Research Center, Rajaie Cardiovascular Medical and Research Center of Iran University of Medical Sciences for their scientific support.

Author contributions

M.N. and M.F. conceived of the presented idea. M.N. developed the theory and performed the computations. M.A.M. and M.O.M. verified the analytical methods. M.O.M. encouraged M.N. to investigate and supervised the findings of this work. All authors discussed the results and contributed to the final manuscript.

Data availability

The datasets generated and/or analyzed during the current study are not publicly available due authors are currently analyzing for further work but are available from the corresponding author on reasonable request.

Compliance with ethical standards

Conflict of interest: The author has no conflicts of interest or competing for financial interests to declare. This

research received no grant funding or writing assistants from agencies of the public commercial, or not-for-profit sectors.

Ethics statements: Ethics approval, consent to participate, consent for publication, and availability of data and material are not applicable for this manuscript.

References

- [1] M. Dehghani, Y. Kamali, F. Jamshidi, M.A. Shiri, M. Nozari, Contribution of H_2O_2 in ultrasonic systems for degradation of DR-81 dye from aqueous solutions, *Desal. Water Treat.*, 107 (2018) 332–339.
- [2] M. Dehghani, M. Nozari, I. Golkari, N. Rostami, M.A. Shiri, Adsorption and kinetic studies of hexavalent chromium by dehydrated *Scrophularia striata* stems from aqueous solutions, *Desal. Water Treat.*, 125 (2018) 81–92.
- [3] M. Dehghani, M. Nozari, I. Golkari, N. Rostami, M.A. Shiri, Adsorption of mercury(II) from aqueous solutions using dried *Scrophularia striata* stems: adsorption and kinetic studies, *Desal. Water Treat.*, 203 (2020) 279–291.
- [4] M. Dehghani, M. Nozari, A. Fakhraei Fard, M. Ansari Shiri, N. Shamsedini, Direct red 81 adsorption on iron filings from aqueous solutions; kinetic and isotherm studies, *Environ. Technol.*, 40 (2019) 1705–1713.
- [5] M. Dehghani, M.A. Shiri, S. Shahsavani, N. Shamsedini, M. Nozari, Removal of Direct Red 81 dye from aqueous solution using neutral soil containing copper, *Desal. Water Treat.*, 86 (2017) 213–220.
- [6] M. Malakootian, N. Olama, A. Nasiri, Photocatalytic degradation of metronidazole from aquatic solution by TiO_2 -doped Fe^{3+} nano-photocatalyst, *Int. J. Environ. Sci. Technol.*, 16 (2019) 4275–4284.
- [7] Y.Y. Sun, Q.Y. Yue, B.Y. Gao, Y. Gao, X. Xu, Q. Li, Y. Wang, Adsorption and cosorption of ciprofloxacin and Ni(II) on activated carbon-mechanism study, *J. Taiwan. Inst. Chem. Eng.*, 45 (2014) 681–688.
- [8] J.H. Jin, Z.H. Yang, W.P. Xiong, Y.Y. Zhou, R. Xu, Y.R. Zhang, J. Cao, X. Li, C.Y. Zhou, Cu and Co nanoparticles co-doped MIL-101 as a novel adsorbent for efficient removal of tetracycline from aqueous solutions, *Sci. Total Environ.*, 650 (2019) 408–418.
- [9] M. Malakootian, M. Ahmadian, Ciprofloxacin removal by electro-activated persulfate in aqueous solution using iron electrodes, *Appl. Water Sci.*, 9 (2019) 2–10.
- [10] N. Amirmahani, H. Mahdizadeh, M. Malakootian, A. Pardakhty, N.O. Mahmoodi, Evaluating nanoparticles decorated on $Fe_3O_4@SiO_2$ -schiff base ($Fe_3O_4@SiO_2$ -APTMS-HBA) in adsorption of ciprofloxacin from aqueous environments, *J. Inorg. Organomet. Polym. Mater.*, 30 (2020) 1–12, doi: 10.1007/s10904-020-01499-5.
- [11] A.A. Alswat, M.B. Ahmad, M.Z. Hussein, N.A. Ibrahim, T.A. Saleh, Copper oxide nanoparticles-loaded zeolite and its characteristics and antibacterial activities, *J. Mater. Sci. Technol.*, 33 (2017) 889–896.
- [12] A.A. Alswat, M.B. Ahmad, T.A. Saleh, Preparation and characterization of zeolite\zinc oxide-copper oxide nanocomposite: antibacterial activities, *Colloids Interface Sci.*, 16 (2017) 19–24.
- [13] A.A. Alswat, M.B. Ahmad, T.A. Saleh, M.Z.B. Hussein, N.A. Ibrahim, Effect of zinc oxide amounts on the properties and antibacterial activities of zeolite/zinc oxide nanocomposite, *Mater. Sci. Eng.*, 68 (2016) 505–511.
- [14] T.A. Saleh, Nanomaterials: classification, properties, and environmental toxicities, *Environ. Technol. Innovation*, 20 (2020) 101067, doi: 10.1016/j.eti.2020.101067.
- [15] A.S. Giri, A.K. Golder, Ciprofloxacin degradation from aqueous solution by Fenton oxidation: reaction kinetics and degradation mechanisms, *RSC Adv.*, 4 (2014) 6738–6745.
- [16] M. Malakootian, M. Ahmadian, Removal of ciprofloxacin from aqueous solution by electro-activated persulfate oxidation using aluminum electrodes, *Water Sci. Technol.*, 80 (2019) 587–596.
- [17] L.J.M. Githinji, M.K. Musey, R.O. Ankumah, Evaluation of the fate of ciprofloxacin and amoxicillin in domestic wastewater, *Water Air Soil Pollut.*, 219 (2011) 191–201.
- [18] E.M. Golet, A.C. Alder, W. Giger, Environmental exposure and risk assessment of fluoroquinolone antibacterial agents in wastewater and river water of the Glatt Valley Watershed, Switzerland, *Environ. Sci. Technol.*, 36 (2002) 3645–3651.
- [19] W.-T. Jiang, P.-H. Chang, Y.-S. Wang, Y.L. Tsai, J.-S. Jean, Z.H. Li, K. Krukowski, Removal of ciprofloxacin from water by birnessite, *J. Hazard. Mater.*, 250 (2013) 362–369.
- [20] O.A. Alsager, M.N. Alnajrani, H.A. Abuelizz, I.A. Aldaghmani, Removal of antibiotics from water and waste milk by ozonation: kinetics, byproducts, and antimicrobial activity, *Ecotoxicol. Environ. Saf.*, 158 (2018) 114–122.
- [21] T.A. Gad-Allah, M.E.M. Ali, M.I. Badawy, Photocatalytic oxidation of ciprofloxacin under simulated sunlight, *J. Hazard. Mater.*, 186 (2011) 751–755.
- [22] A. Hassani, A. Khataee, M. Fathinia, S. Karaca, Photocatalytic ozonation of ciprofloxacin from aqueous solution using TiO_2 /MMT nanocomposite: nonlinear modeling and optimization of the process via artificial neural network integrated genetic algorithm, *Process Saf. Environ. Prot.*, 116 (2018) 365–376.
- [23] T.G. Vasconcelos, D.M. Henriques, A. Konig, A.F. Martins, K. Kummerer, Photo-degradation of the antimicrobial ciprofloxacin at high pH: identification and biodegradability assessment of the primary by-products, *Chemosphere*, 76 (2009) 487–493.
- [24] H. Li, D. Zhang, X. Han, B. Xing, Adsorption of antibiotic ciprofloxacin on carbon nanotubes: pH dependence and thermodynamics, *Chemosphere*, 95 (2014) 150–155.
- [25] M. Malakootian, A. Nasiri, H. Mahdizadeh, Preparation of $CoFe_2O_4$ /activated carbon@chitosan as a new magnetic nanobiocomposite for adsorption of ciprofloxacin in aqueous solutions, *Water Sci. Technol.*, 78 (2018) 2158–2170.
- [26] Y. Wang, C.C. Shen, M.M. Zhang, B.T. Zhang, Y.G. Yu, The electrochemical degradation of ciprofloxacin using a SnO_2 -Sb/Ti anode: influencing factors, reaction pathways and energy demand, *Chem. Eng. J.*, 296 (2016) 79–89.
- [27] M.Sh. Yahya, N. Oturan, K. El Karbane, C.T. Aravindakumar, M.A. Oturan, Oxidative degradation study on antimicrobial agent ciprofloxacin by electro-fenton process: kinetics and oxidation products, *Chemosphere*, 117 (2014) 447–454.
- [28] A. Rahdar, S. Rahdar, S. Ahmadi, J. Fu, Adsorption of ciprofloxacin from aqueous environment by using synthesized nanoceria, *Ecol. Chem. Eng.*, 26 (2019) 299–311.
- [29] N. Genç, D. Esra Can, M. Yurtsever, Bentonite for ciprofloxacin removal from aqueous solution, *Water Sci. Technol.*, 68 (2013) 848–855.
- [30] S.T. Danalioğlu, O.K. Kuyumcu, M.A. Salam, S.S. Bayazit, Chitosan grafted SiO_2 - Fe_3O_4 nanoparticles for removal of antibiotics from water, *Environ. Sci. Pollut. Res.*, 25 (2018) 36661–36670.
- [31] W.R.D.N. Sousa, A.R. Oliveira, J.F. Cruz Filho, T.C.M. Dantas, A.G.D. Santos, V.P.S. Caldeira, G.E. Luz Jr., Ciprofloxacin adsorption on ZnO supported on SBA-15, *Water Air Soil Pollut.*, 229 (2018) 1–12.
- [32] S. Yadav, N. Goel, V. Kumar, K. Tikoo, S. Singhal, Removal of fluoroquinolone from aqueous solution using graphene oxide: experimental and computational elucidation, *Environ. Sci. Pollut. Res.*, 25 (2018) 2942–2957.
- [33] M.E. Roca Jalil, F. Toschi, M. Baschini, K. Sapag, Silica pillared montmorillonites as possible adsorbents of antibiotics from water media, *Appl. Sci.*, 8 (2018) 1403, doi: 10.3390/app 8081403.
- [34] E. Weidemann, M. Niinipuu, J. Fick, S. Jansson, Using carbonized low-cost materials for removal of chemicals of environmental concern from water, *Environ. Sci. Pollut. Res.*, 25 (2018) 15793–15801.
- [35] J.A. García-Alonso, B.C. Sulbarán-Rangel, E.R. Bandala, J. del Real-Olvera, Adsorption and kinetic studies of the removal of ciprofloxacin from aqueous solutions by diatomaceous earth, *Desal. Water Treat.*, 162 (2019) 331–340.

- [36] H. Fan, Y. Ma, J. Wan, Y. Wang, Z. Li, Y. Chen, Adsorption properties and mechanisms of novel biomaterials from banyan aerial roots via simple modification for ciprofloxacin removal, *Sci. Total Environ.*, 708 (2019) 134630, doi: 10.1016/j.scitotenv.2019.134630.
- [37] C. Dube, R. Tandlich, B. Wilhelmi, Adsorptive removal of ciprofloxacin and isoniazid from aqueous solution, *Nova Biotechnol. Chim.*, 17 (2018) 16–28.
- [38] F. Yu, D. Chen, J. Ma, Adsorptive removal of ciprofloxacin by ethylene diaminetetraacetic acid/β-cyclodextrin composite from aqueous solution, *New J. Chem.*, 42 (2018) 2216–2223.
- [39] N. Dhiman, N. Sharma, Batch adsorption studies on the removal of ciprofloxacin hydrochloride from aqueous solution using ZnO nanoparticles and groundnut (*Arachis hypogaea*) shell powder: a comparison, *Indian Chem. Eng.*, 61 (2019) 67–76.
- [40] N.A. Elessawy, M. Elnoubi, M.H. Gouda, H.A. Hamad, N.A. Taha, M. Gouda, M.S. Mohy Eldin, Ciprofloxacin removal using magnetic fullerene nanocomposite obtained from sustainable PET bottle wastes: adsorption process optimization, kinetics, isotherm, regeneration and recycling studies, *Chemosphere*, 239 (2020) 124728, doi: 10.1016/j.chemosphere.2019.124728.
- [41] A. Avci, İ. İnci, N. Baylan, A comparative adsorption study with various adsorbents for the removal of ciprofloxacin hydrochloride from water, *Water Air Soil Pollut.*, 230 (2019) 2–9.
- [42] N.F. Wang, W.L. Xiao, B.H. Niu, W.Z. Duan, L. Zhou, Y. Zheng, Highly efficient adsorption of fluoroquinolone antibiotics using chitosan derived granular hydrogel with 3D structure, *J. Mol. Liq.*, 281 (2019) 307–314.
- [43] Z. Li, M. Ma, S. Zhang, Z. Zhang, L. Zhou, J. Yun, R. Liu, Efficient removal of ciprofloxacin from aqueous solution by MIL-101(Cr)-HSO₄⁻: the enhanced electrostatic interaction, *J. Porous Mater.*, 27 (2019) 189–204.
- [44] M.Y. Nassar, I.S. Ahmed, M.A. Raya, A facile and tunable approach for synthesis of pure silica nanostructures from rice husk for the removal of ciprofloxacin drug from polluted aqueous solutions, *J. Mol. Liq.*, 282 (2019) 251–263.
- [45] C.I. Tay, S.T. Ong, Guava leaves as adsorbent for the removal of emerging pollutant: ciprofloxacin from aqueous solution, *J. Phys. Sci.*, 30 (2019) 137–156.
- [46] R. Cheng, H. Li, Z. Liu, C. Du, Halloysite nanotubes as an effective and recyclable adsorbent for removal of low-concentration antibiotics ciprofloxacin, *Minerals*, 8 (2018) 387, doi: 10.3390/min8090387.
- [47] Y. Gan, M. Zhang, J. Xiong, J. Zhu, W. Li, C. Zhang, G. Cheng, Impact of Cu particles on adsorption and photocatalytic capability of mesoporous Cu@TiO₂ hybrid towards ciprofloxacin antibiotic removal, *J. Taiwan. Inst. Chem. Eng.*, 96 (2019) 229–242.
- [48] M.E. Roca Jalil, M. Baschini, K. Sapag, Influence of pH and antibiotic solubility on the removal of ciprofloxacin from aqueous media using montmorillonite, *Appl. Clay Sci.*, 114 (2015) 69–76.
- [49] S.K. Bajpai, M. Bhowmik, Poly(acrylamide-co-itaconic acid) as a potential ion-exchange sorbent for effective removal of antibiotic drug-ciprofloxacin from aqueous solution, *J. Macromol. Sci., Pure Appl. Chem.*, 48 (2011) 108–118.
- [50] N. Genç, Removal of antibiotic ciprofloxacin hydrochloride from water by Kandira stone: kinetic models and thermodynamic, *Global NEST J.*, 17 (2015) 498–507.
- [51] T.S. Khokhar, F.N. Memon, A.A. Memon, F. Durmaz, S. Memon, Q.K. Panhwar, S. Muneer, Removal of ciprofloxacin from aqueous solution using wheat bran as adsorbent, *Sep. Sci. Technol.*, 54 (2019) 1278–1288.
- [52] M.E.R. Jalil, M. Baschini, K. Sapag, Removal of ciprofloxacin from aqueous solutions using pillared clays, *Materials*, 10 (2017) 1345, doi: 10.3390/ma10121345.
- [53] C. Zheng, H. Zheng, C. Hu, Y. Wang, Y. Wang, C. Zhao, W. Ding, Q. Sun, Structural design of magnetic biosorbents for the removal of ciprofloxacin from water, *Bioresour. Technol.*, 296 (2020) 122288, doi: 10.1016/j.biortech.2019.122288.
- [54] S. Rahdar, A. Rahdar, C.A. Igwegbe, F. Moghaddam, S. Ahmadi, Synthesis and physical characterization of nickel oxide nanoparticles and its application study in the removal of ciprofloxacin from contaminated water by adsorption: equilibrium and kinetic studies, *Desal. Water Treat.*, 141 (2019) 386–393.
- [55] S. Karoui, R. Ben Arfi, K. Mougin, A. Ghorbal, A.A. Assadi, A. Amrane, Synthesis of novel biocomposite powder for simultaneous removal of hazardous ciprofloxacin and methylene blue: Central composite design, kinetic and isotherm studies using Brouers-Sotolongo family models, *J. Hazard. Mater.*, 387 (2019) 121675, doi: 10.1016/j.jhazmat.2019.121675.
- [56] V. Arya, L. Philip, Adsorption of pharmaceuticals in water using Fe₃O₄ coated polymer clay composite, *Microporous Mesoporous Mater.*, 232 (2016) 273–280.
- [57] C. Rizzo, S. Marullo, N.T. Dintcheva, F. D'Anna, Carbon nanomaterial doped ionic liquid gels for the removal of pharmaceutically active compounds from water, *Molecules*, 24 (2019) 2788, doi: 10.3390/molecules24152788.
- [58] C.J. Wang, Z. Li, W.T. Jiang, J.S. Jean, C.C. Liu, Cation exchange interaction between antibiotic ciprofloxacin and montmorillonite, *J. Hazard. Mater.*, 183 (2010) 309–314.
- [59] M. Nazraz, Y. Yamini, H. Asiabi, Chitosan-based sorbent for efficient removal and extraction of ciprofloxacin and norfloxacin from aqueous solutions, *Microchim. Acta*, 186 (2019) 459, doi: 10.1007/s00604-019-3563-x.
- [60] Z.-W. Zeng, X.-F. Tan, Y.-G. Liu, S.-R. Tian, G.-M. Zeng, L.-H. Jiang, S.-B. Liu, J. Li, N. Liu, Z.-H. Yin, Comprehensive adsorption studies of doxycycline and ciprofloxacin antibiotics by biochars prepared at different temperatures, *Front. Chem.*, 6 (2018) 80, doi: 10.3389/fchem.2018.00080.
- [61] R. Rostamian, H. Behnejad, A comprehensive adsorption study and modeling of antibiotics as a pharmaceutical waste by graphene oxide nanosheets, *Ecotoxicol. Environ. Saf.*, 147 (2018) 117–123.
- [62] J. Gao, X. Zhang, S. Xu, F. Tan, X. Li, Y. Zhang, Z. Qu, X. Quan, J. Liu, Clickable periodic mesoporous organosilicas: synthesis, click reactions, and adsorption of antibiotics, *Chemistry*, 20 (2014) 1957–1963.
- [63] Y. Wu, Y. Tang, L. Li, P. Liu, X. Li, W. Chen, Y. Xue, The correlation of adsorption behavior between ciprofloxacin hydrochloride and the active sites of Fe-doped MCM-41, *Front. Chem.*, 6 (2018) 17, doi: 10.3389/fchem.2018.00017.
- [64] M.L. Soran, O. Opris, I. Lung, I. Kacso, A.S. Porav, M. Stan, The efficiency of the multi-walled carbon nanotubes used for antibiotics removal from wastewaters generated by animal farms, *Environ. Sci. Pollut. Res. Int.*, 24 (2017) 16396–16406.
- [65] S. Wang, X. Li, H. Zhao, X. Quan, S. Chen, H. Yu, Enhanced adsorption of ionizable antibiotics on activated carbon fiber under electrochemical assistance in continuous-flow modes, *Water Res.*, 134 (2018) 162–169.
- [66] A. Dehghan, A.A. Mohammadi, M. Yousefi, A.A. Najafpoor, M. Shams, S. Rezania, Enhanced kinetic removal of ciprofloxacin onto metal-organic frameworks by sonication, process optimization and metal leaching study, *Nanomaterials*, 9 (2019) 1422, doi: 10.3390/nano9101422.
- [67] M.Z. Afzal, X.F. Sun, J. Liu, C. Song, S.G. Wang, A. Javed, Enhancement of ciprofloxacin sorption on chitosan/biochar hydrogel beads, *Sci. Total Environ.*, 639 (2018) 560–569.
- [68] J.R. Li, Y.X. Wang, X. Wang, B. Yuan, M.L. Fu, Intercalation and adsorption of ciprofloxacin by layered chalcogenides and kinetics study, *J. Colloid Interface Sci.*, 453 (2015) 69–78.
- [69] S.F. Soares, M.J. Rocha, M. Ferro, C.O. Amorim, J.S. Amaral, T. Trindade, A.L. Daniel-da-Silva, Magnetic nanosorbents with siliceous hybrid shells of alginic acid and carrageenan for removal of ciprofloxacin, *Int. J. Biol. Macromol.*, 139 (2019) 827–841.
- [70] H. Rasoulzadeh, A. Mohseni-Bandpei, M. Hosseini, M. Safari, Mechanistic investigation of ciprofloxacin recovery by magnetite-imprinted chitosan nanocomposite: isotherm, kinetic, thermodynamic and reusability studies, *Int. J. Biol. Macromol.*, 133 (2019) 712–721.
- [71] Y. Privar, D. Shashura, A. Pestov, E. Modin, A. Baklykov, D. Marinin, S. Bratskaya, Metal-chelate sorbents based on carboxyalkylchitosans: ciprofloxacin uptake by Cu(II) and

- Al(III)-chelated cryogels of N-(2-carboxyethyl)chitosan, *Int. J. Biol. Macromol.*, 131 (2019) 806–811.
- [72] W.T. Jiang, P.H. Chang, Y.L. Tsai, Z.H. Li, Halloysite nanotubes as a carrier for the uptake of selected pharmaceuticals, *Microporous Mesoporous Mater.*, 220 (2016) 298–307.
- [73] V.P. Singh, M. Sharma, R. Vaish, Multifunctional diesel exhaust emission soot coated sponge for water treatment, *Environ. Sci. Pollut. Res. Int.*, 26 (2019) 8148–8156.
- [74] A. Ashiq, N.M. Adasooriya, B. Sarkar, A.U. Rajapaksha, Y.S. Ok, M. Vithanage, Municipal solid waste biochar–montmorillonite composite for the removal of antibiotic ciprofloxacin from aqueous media, *J. Environ. Manage.*, 236 (2019) 428–435.
- [75] W.N. Ge, Z.P. Zhou, P. Zhang, Q.F. Zhang, Z. Cao, R.L. Zhang, Y.S. Yan, J.D. Dai, Graphene oxide template-confined fabrication of hierarchical porous carbons derived from lignin for ultrahigh-efficiency and fast removal of ciprofloxacin, *J. Ind. Eng. Chem.*, 66 (2018) 456–467.
- [76] A. Gouza, S. Saeiabi, M. El Karbane, S. Masse, G. Laurent, A. Rami, A. Saeiabi, A. Laghzizil, T. Coradin, Oil shale powders and their interactions with ciprofloxacin, ofloxacin, and oxytetracycline antibiotics, *Environ. Sci. Pollut. Res. Int.*, 24 (2017) 25977–25985.
- [77] M.C. Ncibi, M. Sillanpaa, Optimized removal of antibiotic drugs from aqueous solutions using single, double and multi-walled carbon nanotubes, *J. Hazard. Mater.*, 298 (2015) 102–110.
- [78] M.-F. Li, Y.-G. Liu, S.-B. Liu, G.-M. Zeng, X.-J. Hu, X.-F. Tan, L.-H. Jiang, N. Liu, J. Wen, X.-H. Liu, Performance of magnetic graphene oxide/diethylenetriaminepentaacetic acid nanocomposite for the tetracycline and ciprofloxacin adsorption in single and binary systems, *J. Colloid Interface Sci.*, 521 (2018) 150–159.
- [79] J. Nogueira, M. António, S.M. Mikhalev, S. Fateixa, T. Trindade, A.L. Daniel-da-Silva, Porous carrageenan-derived carbons for efficient ciprofloxacin removal from water, *Nanomaterials*, 8 (2018) 1004, doi: 10.3390/nano8121004.
- [80] Y.X. Wang, H.H. Ngo, W.S. Guo, Preparation of a specific bamboo based activated carbon and its application for ciprofloxacin removal, *Sci. Total Environ.*, 533 (2015) 32–39.
- [81] L. Liu, X. Chen, Z. Wang, S. Lin, Removal of aqueous fluoroquinolones with multi-functional activated carbon (MFAC) derived from recycled long-root *Eichhornia crassipes*: batch and column studies, *Environ. Sci. Pollut. Res. Int.*, 26 (2019) 34345–34356.
- [82] W. Huang, J. Chen, J. Zhang, Removal of ciprofloxacin from aqueous solution by rabbit manure biochar, *Environ. Technol.*, 41 (2018) 1380–1390.
- [83] H. Chen, B. Gao, H. Li, Removal of sulfamethoxazole and ciprofloxacin from aqueous solutions by graphene oxide, *J. Hazard. Mater.*, 282 (2015) 201–207.
- [84] A. Ashiq, B. Sarkar, N. Adasooriya, J. Walpita, A.U. Rajapaksha, Y.S. Ok, M. Vithanage, Sorption process of municipal solid waste biochar–montmorillonite composite for ciprofloxacin removal in aqueous media, *Chemosphere*, 236 (2019) 124384, doi: 10.1016/j.chemosphere.2019.124384.
- [85] J. Jin, T. Feng, R. Gao, Y. Ma, W. Wang, Q. Zhou, A. Li, Ultrahigh selective adsorption of zwitterionic PPCPs both in the absence and presence of humic acid: performance and mechanism, *J. Hazard. Mater.*, 348 (2018) 117–124.
- [86] S. Indherjith, S. Karthikeyan, J.H.R. Monica, K.K. Kumar, Graphene oxide & reduced graphene oxide polysulfone nanocomposite pellets: an alternative adsorbent of antibiotic pollutant-ciprofloxacin, *Sep. Sci. Technol.*, 54 (2019) 667–674.
- [87] J.A. Perini, B.F. Silva, R.F. Nogueira, Zero-valent iron mediated degradation of ciprofloxacin – assessment of adsorption, operational parameters and degradation products, *Chemosphere*, 117 (2014) 345–352.
- [88] C.H. Liang, X.D. Zhang, P. Feng, H.X. Chai, Y.M. Huang, ZIF-67 derived hollow cobalt sulfide as superior adsorbent for effective adsorption removal of ciprofloxacin antibiotics, *Chem. Eng. J.*, 344 (2018) 95–104.
- [89] S.Q. Li, X.D. Zhang, Y.M. Huang, Zeolitic imidazolate framework-8 derived nanoporous carbon as an effective and recyclable adsorbent for removal of ciprofloxacin antibiotics from water, *J. Hazard. Mater.*, 321 (2017) 711–719.
- [90] D. Zide, O. Fatoki, O. Oputu, B. Opeolu, S. Nelana, O. Olatunji, Zeolite ‘adsorption’ capacities in aqueous acidic media; The role of acid choice and quantification method on ciprofloxacin removal, *Microporous Mesoporous Mater.*, 255 (2018) 226–241.
- [91] J. Ma, M.X. Yang, F. Yu, J. Zheng, Water-enhanced removal of ciprofloxacin from water by porous graphene hydrogel, *Sci. Rep.*, 5 (2015) 10, doi: 10.1038/srep13578.
- [92] R. Rostamian, H. Behnejad, A unified platform for experimental and quantum mechanical study of antibiotic removal from water, *J. Water Process. Eng.*, 17 (2017) 207–215.
- [93] Y. Zhuang, F. Yu, J. Ma, J.H. Chen, Graphene as a template and structural scaffold for the synthesis of a 3D porous bio-adsorbent to remove antibiotics from water, *RSC Adv.*, 5 (2015) 27964–27969.
- [94] C.L. Zhang, G.L. Qiao, F. Zhao, Y. Wang, Thermodynamic and kinetic parameters of ciprofloxacin adsorption onto modified coal fly ash from aqueous solution, *J. Mol. Liq.*, 163 (2011) 53–56.
- [95] Y.L. Tang, H.G. Guo, L. Xiao, S.L. Yu, N.Y. Gao, Y.L. Wang, Synthesis of reduced graphene oxide/magnetite composites and investigation of their adsorption performance of fluoroquinolone antibiotics, *Colloids Surf., A*, 424 (2013) 74–80.
- [96] J. Wang, J.D. Dai, M.J. Meng, Z.L. Song, J.M. Pan, Y.S. Yan, C.X. Li, Surface molecularly imprinted polymers based on yeast prepared by atom transfer radical emulsion polymerization for selective recognition of ciprofloxacin from aqueous medium, *J. Appl. Polym. Sci.*, 131 (2014) 10, doi: 10.1002/app.40310.
- [97] D. Liu, W.W. Lei, S. Qin, K.D. Klika, Y. Chen, Superior adsorption of pharmaceutical molecules by highly porous BN nanosheets, *Phys. Chem. Chem. Phys.*, 18 (2016) 84–88.
- [98] S. Ahmadi, A. Banach, F.K. Mostafapour, D. Balarak, Study survey of cupric oxide nanoparticles in removal efficiency of ciprofloxacin antibiotic from aqueous solution: adsorption isotherm study, *Desal. Water Treat.*, 89 (2017) 297–303.
- [99] X. Peng, F. Hu, H. Dai, Q. Xiong, C. Xu, Study of the adsorption mechanisms of ciprofloxacin antibiotics onto graphitic ordered mesoporous carbons, *J. Taiwan. Inst. Chem. Eng.*, 65 (2016) 472–481.
- [100] J. Li, G.W. Yu, L.J. Pan, C.X. Li, F.T. You, S.Y. Xie, Y. Wang, J.L. Ma, X.F. Shang, Study of ciprofloxacin removal by biochar obtained from used tea leaves, *J. Environ. Sci.*, 73 (2018) 20–30.
- [101] P.V.F. de Sousa, A.F. de Oliveira, A.A. da Silva, B.G. Vaz, R.P. Lopes, Study of ciprofloxacin degradation by zero-valent copper nanoparticles, *Chem. Pap.*, 73 (2019) 249–260.
- [102] M. Wang, G. Li, L.H. Huang, J. Xue, Q. Liu, N. Bao, J. Huang, Study of ciprofloxacin adsorption and regeneration of activated carbon prepared from *Enteromorpha prolifera* impregnated with H_3PO_4 and sodium benzenesulfonate, *Ecotoxicol. Environ. Saf.*, 139 (2017) 36–42.
- [103] F. Reynaud, N. Tsapis, M. Deyme, T.G. Vasconcelos, C. Gueutin, S.S. Gutierrez, A.R. Pohlmann, E. Fattal, Spray-dried chitosan-metal microparticles for ciprofloxacin adsorption: kinetic and equilibrium studies, *Soft Matter*, 7 (2011) 7304–7312.
- [104] A. Septian, S. Oh, W.S. Shin, Sorption of antibiotics onto montmorillonite and kaolinite: competition modelling, *Environ. Technol.*, 40 (2019) 2940–2953.
- [105] G.Z. Liu, Z.L. Zhu, Y.X. Yang, Y.R. Sun, F. Yu, J. Ma, Sorption behavior and mechanism of hydrophilic organic chemicals to virgin and aged microplastics in freshwater and seawater, *Environ. Pollut.*, 246 (2019) 26–33.
- [106] X.N. Li, S. Chen, X.F. Fan, X. Quan, F. Tan, Y.B. Zhang, J.S. Gao, Adsorption of ciprofloxacin, bisphenol and 2-chlorophenol on electrospun carbon nanofibers: in comparison with powder activated carbon, *J. Colloid Interface Sci.*, 447 (2015) 120–127.
- [107] A. Pardo, H. Garcia, P. Ramirez, M.A. Carrillo-Alvarado, K.S. Krishna, N. Dominguez, M.T. Islam, H.Y. Wang, J.C. Noveron, Self-regenerating photocatalytic hydrogel for the adsorption and decomposition of methylene blue and antibiotics in water, *Environ. Technol. Innovation*, 11 (2018) 321–327.

- [108] J. Ma, Y.R. Sun, F. Yu, Self-assembly and controllable synthesis of graphene hydrogel adsorbents with enhanced removal of ciprofloxacin from aqueous solutions, *RSC Adv.*, 6 (2016) 83982–83993.
- [109] X.J. Zhang, X.Y. Gao, P.W. Huo, Y.S. Yan, Selective adsorption of micro ciprofloxacin by molecularly imprinted functionalized polymers appended onto ZnS, *Environ. Technol.*, 33 (2012) 2019–2025.
- [110] I. Brnardić, L. Ćurković, T. Sofilić, D.M. Pavlović, G. Matijašić, I. Grčić, A. Radenović Removal of heavy metals and pharmaceuticals from contaminated water using waste sludge – kinetics and mechanisms, *Clean–Soil Air Water*, 45 (2017) 9, doi: 10.1002/clen.201600509.
- [111] B.P. Zhang, X.L. Han, P.J. Gu, S.Q. Fang, J. Bai, Response surface methodology approach for optimization of ciprofloxacin adsorption using activated carbon derived from the residue of desilicated rice husk, *J. Mol. Liq.*, 238 (2017) 316–325.
- [112] Y.R. Sun, Y.X. Yang, M.X. Yang, F. Yu, J. Ma, Response surface methodological evaluation and optimization for adsorption removal of ciprofloxacin onto graphene hydrogel, *J. Mol. Liq.*, 284 (2019) 124–130.
- [113] H.B. Li, W.H. Wu, X.X. Hao, S. Wang, M.Y. You, X.Z. Han, Q. Zhao, B.S. Xing, Removal of ciprofloxacin from aqueous solutions by ionic surfactant-modified carbon nanotubes, *Environ. Pollut.*, 243 (2018) 206–217.
- [114] K. Zheng, X.Y. Zheng, F. Yu, J. Ma, Removal of ciprofloxacin from aqueous solution using long TiO₂ nanotubes with a high specific surface area, *RSC Adv.*, 6 (2016) 3625–3631.
- [115] S.T. Danalioglu, S.S. Bayazit, O. Kerkez, B.G. Alhogbi, M.A. Salam, Removal of ciprofloxacin from aqueous solution using humic acid- and levulinic acid-coated Fe₃O₄ nanoparticles, *Chem. Eng. Res. Des.*, 123 (2017) 259–267.
- [116] L.S. Yi, G.W. Liang, W.L. Xiao, W.Z. Duan, A.Q. Wang, Y. Zheng, Rapid nitrogen-rich modification of *Calotropis gigantea* fiber for highly efficient removal of fluoroquinolone antibiotics, *J. Mol. Liq.*, 256 (2018) 408–415.
- [117] Y.Y. Shao, P. Zhao, Q.Y. Yue, Y.W. Wu, B.Y. Gao, W.J. Kong, Preparation of wheat straw-supported nanoscale zero-valent iron and its removal performance on ciprofloxacin, *Ecotoxicol. Environ. Saf.*, 158 (2018) 100–107.
- [118] J.M. Chaba, P.N. Nomngongo, Preparation of V₂O₅–ZnO coated carbon nanofibers: application for removal of selected antibiotics in environmental matrices, *J. Water Process Eng.*, 23 (2018) 50–60.
- [119] S.S. Bayazit, S.T. Danalioglu, M.A. Salam, O.K. Kuyumcu, Preparation of magnetic MIL-101 (Cr) for efficient removal of ciprofloxacin, *Environ. Sci. Pollut. Res.*, 24 (2017) 25452–25461.
- [120] Y. Yuan, D. Yang, G.B. Mei, X. Hong, J.Y. Wu, J.Y. Zheng, J. Pang, Z.M. Yan, Preparation of konjac glucomannan-based zeolitic imidazolate framework-8 composite aerogels with high adsorptive capacity of ciprofloxacin from water, *Colloids Surf., A*, 544 (2018) 187–195.
- [121] Y.P. Li, C.F. Zeng, C.Q. Wang, L.X. Zhang, Preparation of C@silica core/shell nanoparticles from ZIF-8 for efficient ciprofloxacin adsorption, *Chem. Eng. J.*, 343 (2018) 645–653.
- [122] X.M. Peng, F.P. Hu, J.L. Huang, Y.J. Wang, H.L. Dai, Z.M. Liu, Preparation of a graphitic ordered mesoporous carbon and its application in sorption of ciprofloxacin: kinetics, isotherm, adsorption mechanisms studies, *Microporous Mesoporous Mater.*, 228 (2016) 196–206.
- [123] S. Liu, P.X. Wu, L.F. Yu, L.P. Li, B.N. Gong, N.W. Zhu, Z. Dang, C. Yang, Preparation and characterization of organo-vermiculite based on phosphatidylcholine and adsorption of two typical antibiotics, *Appl. Clay Sci.*, 137 (2017) 160–167.
- [124] W. Ma, J.D. Dai, X.H. Dai, Y.S. Yan, Preparation and characterization of chitosan/kaolin/Fe₃O₄ magnetic microspheres and their application for the removal of ciprofloxacin, *Adsorpt. Sci. Technol.*, 32 (2014) 775–790.
- [125] J. Dong, F.-F. Xu, Z. Liu, H.-Y. Yu, Y. Yan, Y.-X. Li, Porous covalent organic gels: design, synthesis and fluoroquinolones adsorption, *ChemistrySelect*, 3 (2018) 13624–13628.
- [126] E.J. Cao, W.Z. Duan, A.Q. Wang, Y. Zheng, Oriented growth of poly(m-phenylenediamine) on *Calotropis gigantea* fiber for rapid adsorption of ciprofloxacin, *Chemosphere*, 171 (2017) 223–230.
- [127] Y. Gao, Q.Y. Yue, B.Y. Gao, Y.Y. Sun, Optimization preparation of activated carbon from *Enteromorpha prolifera* using response surface methodology and its adsorption studies of fluoroquinolone antibiotics, *Desal. Water Treat.*, 55 (2015) 624–636.
- [128] X. Liu, Y.B. Wan, P.L. Liu, L. Zhao, W.H. Zou, Optimization of process conditions for preparation of activated carbon from waste *Salix psammophila* and its adsorption behavior on fluoroquinolone antibiotics, *Water Sci. Technol.*, 77 (2018) 2555–2565.
- [129] H. Mandizadeh, M. Malakootian, Optimization of ciprofloxacin removal from aqueous solutions by a novel semi-fluid Fe/charcoal micro-electrolysis reactor using response surface methodology, *Process Saf. Environ. Prot.*, 123 (2019) 299–308.
- [130] X.N. Wei, C.L. Ou, S.S. Fang, X.C. Zheng, G.P. Zheng, X.X. Guan, One-pot self-assembly of 3D CdS-graphene aerogels with superior adsorption capacity and photocatalytic activity for water purification, *Powder Technol.*, 345 (2019) 213–222.
- [131] Y. Zhou, S.R. Cao, C.X. Xi, X.L. Li, L. Zhang, G.M. Wang, Z.Q. Chen, A novel Fe₃O₄/graphene oxide/citrus peel-derived bio-char based nanocomposite with enhanced adsorption affinity and sensitivity of ciprofloxacin and sparfloxacin, *Bioresour. Technol.*, 292 (2019) 121951, doi: 10.1016/j.biortech.2019.121951.
- [132] Y.X. Wang, K. Gupta, J.R. Li, B.L. Yuan, J.C.E. Yang, M.L. Fu, Novel chalcogenide based magnetic adsorbent KMS-1/L-Cystein/Fe₃O₄ for the facile removal of ciprofloxacin from aqueous solution, *Colloids Surf., A*, 538 (2018) 378–386.
- [133] X.N. Zhang, X.Y. Lin, H.L. Ding, Y. He, H. Yang, Y. Chen, X.Y. Chen, X.G. Luo, Novel alginate particles decorated with nickel for enhancing ciprofloxacin removal: characterization and mechanism analysis, *Ecotoxicol. Environ. Saf.*, 169 (2019) 392–401.
- [134] J.A. Garcia-Alonso, F. Zurita-Martinez, C.A. Guzman-Gonzalez, J. Del Real-Olvera, B.C. Sulbaran-Rangel, Nanostructured diatomite and its potential for the removal of an antibiotic from water, *Bioinspired Biomimetic Nanobiomater.*, 7 (2018) 167–173.
- [135] M.J. Ahmed, S.K. Theydan, Fluoroquinolones antibiotics adsorption onto microporous activated carbon from lignocellulosic biomass by microwave pyrolysis, *J. Taiwan. Inst. Chem. Eng.*, 45 (2014) 219–226.
- [136] K. Gupta, J.B. Huo, J.C.E. Yang, M.L. Fu, B.L. Yuan, Z.X. Chen, (MoS₄)₍₂₋₎ intercalated CAMoS(4)center dot LDH material for the efficient and facile sequestration of antibiotics from aqueous solution, *Chem. Eng. J.*, 355 (2019) 637–649.
- [137] H. Chen, B. Gao, L.Y. Yang, L.Q. Ma, Montmorillonite enhanced ciprofloxacin transport in saturated porous media with sorbed ciprofloxacin showing antibiotic activity, *J. Contam. Hydrol.*, 173 (2015) 1–7.
- [138] H.X. Mao, S.K. Wang, J.Y. Lin, Z.S. Wang, J. Ren, Modification of a magnetic carbon composite for ciprofloxacin adsorption, *J. Environ. Sci.*, 49 (2016) 179–188.
- [139] T.V. Tran, D.T.C. Nguyen, H.T.N. Le, T.T.K. Tu, N.D. Le, K.T. Lim, L.G. Bach, T.D. Nguyen, MIL-53 (Fe)-directed synthesis of hierarchically mesoporous carbon and its utilization for ciprofloxacin antibiotic remediation, *J. Environ. Chem. Eng.*, 7 (2019) 102881, doi: 10.1016/j.jece.2019.102881.
- [140] Z.H. Li, H.L. Hong, L.B. Liao, C.J. Ackley, L.A. Schulz, R.A. MacDonald, A.L. Mihelich, S.M. Emard, A mechanistic study of ciprofloxacin removal by kaolinite, *Colloids Surf., B*, 88 (2011) 339–344.
- [141] S. Rakshita, D. Sarkar, E.J. Elzinga, P. Punamiya, R. Datta, Mechanisms of ciprofloxacin removal by nano-sized magnetite, *J. Hazard. Mater.*, 246 (2013) 221–226.
- [142] C.Y. Jiang, X.X. Zhang, X.X. Xu, L.S. Wang, Magnetic mesoporous carbon material with strong ciprofloxacin adsorption removal property fabricated through the calcination of mixed valence Fe based metal-organic framework, *J. Porous Mater.*, 23 (2016) 1297–1304.

- [143] G.G. Wu, J.P. Ma, S. Li, J. Guan, B. Jiang, L.Y. Wang, J.H. Li, X.Y. Wang, L.X. Chen, Magnetic copper-based metal organic framework as an effective and recyclable adsorbent for removal of two fluoroquinolone antibiotics from aqueous solutions, *J. Colloid Interface Sci.*, 528 (2018) 360–371.
- [144] Y.N. Xia, J.C. He, S. Chen, S.Y. Gao, W.T. Wang, P. Lu, Y.Y. Yao, Magnetic Co-based carbon materials derived from core–shell metal-organic frameworks for organic contaminant elimination with peroxyomonosulfates, *Dalton Trans.*, 48 (2019) 10251–10259.
- [145] R.N. Li, Z.W. Wang, X.T. Zhao, X. Li, X.Y. Xie, Magnetic biochar-based manganese oxide composite for enhanced fluoroquinolone antibiotic removal from water, *Environ. Sci. Pollut. Res.*, 25 (2018) 31136–31148.
- [146] A. Konwar, A. Gogoi, D. Chowdhury, Magnetic alginate- Fe_3O_4 hydrogel fiber capable of ciprofloxacin hydrochloride adsorption/separation in aqueous solution, *RSC Adv.*, 5 (2015) 81573–81582.
- [147] X.R. Kong, Y.X. Liu, J.C. Pi, W.H. Li, Q.H.G. Liao, J.G. Shang, Low-cost magnetic herbal biochar: characterization and application for antibiotic removal, *Environ. Sci. Pollut. Res.*, 24 (2017) 6679–6687.
- [148] J.G. Shang, X.R. Kong, L.L. He, W.H. Li, Q.J.H. Liao, Low-cost biochar derived from herbal residue: characterization and application for ciprofloxacin adsorption, *Int. J. Environ. Sci. Technol.*, 13 (2016) 2449–2458.
- [149] D. Balarak, F.K. Mostafapour, A. Joghataei, Kinetics and mechanism of red mud in adsorption of ciprofloxacin in aqueous solution, *Biosci. Biotechnol. Res. Commun.*, 10 (2017) 241–248.
- [150] T.M. Berhane, J. Levy, M.P.S. Krekeler, N.D. Danielson, Kinetic sorption of contaminants of emerging concern by a palygorskite-montmorillonite filter medium, *Chemosphere*, 176 (2017) 231–242.
- [151] M.L.P. Ramos, G. Galaburri, J.A. Gonzalez, C.J. Perez, M.E. Villanueva, G.J. Copello, Influence of GO reinforcement on keratin based smart hydrogel and its application for emerging pollutants removal, *J. Environ. Chem. Eng.*, 6 (2018) 7021–7028.
- [152] L.Q. Li, J.H. Zhao, Y.R. Sun, F. Yu, J. Ma, Ionically cross-linked sodium alginate/kappa-carrageenan double-network gel beads with low-swelling, enhanced mechanical properties, and excellent adsorption performance, *Chem. Eng. J.*, 372 (2019) 1091–1103.
- [153] E. Fries, C. Crouzet, C. Michel, A. Togola, Interactions of ciprofloxacin (CIP), titanium dioxide (TiO_2) nanoparticles and natural organic matter (NOM) in aqueous suspensions, *Sci. Total Environ.*, 563 (2016) 971–976.
- [154] Y.P. Lu, M. Jiang, C.W. Wang, Y.P. Wang, W.B. Yang, Impact of molecular size on two antibiotics adsorption by porous resins, *J. Taiwan. Inst. Chem. Eng.*, 45 (2014) 955–961.
- [155] Z.L. Yan, Y.G. Liu, X.F. Tan, S.B. Liu, G.M. Zeng, L.H. Jiang, M.F. Li, Z. Zhou, S. Liu, X.X. Cai, Immobilization of aqueous and sediment-sorbed ciprofloxacin by stabilized Fe-Mn binary oxide nanoparticles: influencing factors and reaction mechanisms, *Chem. Eng. J.*, 314 (2017) 612–621.
- [156] D.Y. Hu, L.J. Wang, Adsorption of ciprofloxacin from aqueous solutions onto cationic and anionic flax noil cellulose, *Desal. Water Treat.*, 57 (2016) 28436–28449.
- [157] T.M. Berhane, J. Levy, M.P.S. Krekeler, N.D. Danielson, Adsorption of bisphenol A and ciprofloxacin by palygorskite-montmorillonite: effect of granule size, solution chemistry and temperature, *Appl. Clay Sci.*, 132 (2016) 518–527.
- [158] X.B. Xing, J.W. Feng, G.C. Lv, K.N. Song, L.F. Mei, L.B. Liao, X.Y. Wang, B. Xu, Adsorption mechanism of ciprofloxacin from water by synthesized birnessite, *Adv. Mater. Sci. Eng.*, 2015 (2015) 7, doi: 10.1155/2015/148423.
- [159] N. Genc, E.C. Dogan, Adsorption kinetics of the antibiotic ciprofloxacin on bentonite, activated carbon, zeolite, and pumice, *Desal. Water Treat.*, 53 (2015) 785–793.
- [160] D. Balarak, F.K. Mostafapour, H. Azarpira, Adsorption kinetics and equilibrium of ciprofloxacin from aqueous solutions using *Corylus avellana* (hazelnut) activated carbon, *Brit. J. Pharm. Res.*, 13 (2016) 1–14.
- [161] X.M. Peng, F.P. Hu, F.L.Y. Lam, Y.J. Wang, Z.M. Liu, H.L. Dai, Adsorption behavior and mechanisms of ciprofloxacin from aqueous solution by ordered mesoporous carbon and bamboo-based carbon, *J. Colloid Interface Sci.*, 460 (2015) 349–360.
- [162] N. Dhiman, N. Sharma, Removal of ciprofloxacin hydrochloride from aqueous solution using vertical bed and sequential bed columns, *J. Environ. Chem. Eng.*, 6 (2018) 4391–4398.
- [163] Z.R. Li, F.F. Xu, Z. Liu, C.Y. Qin, H. Ren, Y.X. Li, Facile synthesis of novel porous self-assembling hydrogen-bonding covalent organic polymers and their applications towards fluoroquinolone antibiotics adsorption, *RSC Adv.*, 8 (2018) 33516–33522.
- [164] J. Zhang, M.A. Khan, M.Z. Xia, A.M. Abdo, W. Lei, C. Liao, F.Y. Wang, Facile hydrothermal synthesis of magnetic adsorbent $\text{CoFe}_2\text{O}_4/\text{MMT}$ to eliminate antibiotics in aqueous phase: tetracycline and ciprofloxacin, *Environ. Sci. Pollut. Res.*, 26 (2019) 215–226.
- [165] Y. Zhuang, F. Yu, J. Ma, J.H. Chen, Adsorption of ciprofloxacin onto graphene-soy protein biocomposites, *New J. Chem.*, 39 (2015) 3333–3336.
- [166] S.L. Wu, X.D. Zhao, Y.H. Li, C.T. Zhao, Q.J. Du, J.K. Sun, Y.H. Wang, X.J. Peng, Y.Z. Xia, Z.H. Wang, L.H. Xia, Adsorption of ciprofloxacin onto biocomposite fibers of graphene oxide/calcium alginate, *Chem. Eng. J.*, 230 (2013) 389–395.
- [167] S. Das, A. Adak, A. Barui, Fabrication of Montmorillonite impregnated cellulose acetate nanofiber membrane and its use for adsorption of ciprofloxacin, *J. Indian Chem. Soc.*, 96 (2019) 475–479.
- [168] M.K.M. Nodeh, S. Soltani, S. Shahabuddin, H.R. Nodeh, H. Sereshti, Equilibrium, kinetic and thermodynamic study of magnetic polyaniline/graphene oxide based nanocomposites for ciprofloxacin removal from water, *J. Inorg. Organomet. Polym. Mater.*, 28 (2018) 1226–1234.
- [169] Z. Movasaghi, B. Yan, C. Niu, Adsorption of ciprofloxacin from water by pretreated oat hulls: equilibrium, kinetic, and thermodynamic studies, *Ind. Crops Prod.*, 127 (2019) 237–250.
- [170] M.Z. Afzal, R.Y. Yue, X.F. Sun, C. Song, S.G. Wang, Enhanced removal of ciprofloxacin using humic acid modified hydrogel beads, *J. Colloid Interface Sci.*, 543 (2019) 76–83.
- [171] K. Luo, Y. Pang, Q. Yang, D.B. Wang, X. Li, L.P. Wang, M. Lei, J.M. Liu, Enhanced ciprofloxacin removal by sludge-derived biochar: effect of humic acid, *Chemosphere*, 231 (2019) 495–501.
- [172] F. Yu, J. Ma, D.S. Bi, Enhanced adsorptive removal of selected pharmaceutical antibiotics from aqueous solution by activated graphene, *Environ. Sci. Pollut. Res.*, 22 (2015) 4715–4724.
- [173] Y. Zhuang, F. Yu, J. Ma, J.H. Chen, Enhanced adsorption removal of antibiotics from aqueous solutions by modified alginate/graphene double network porous hydrogel, *J. Colloid Interface Sci.*, 507 (2017) 250–259.
- [174] W.Z. Duan, M.H. Li, W.L. Xiao, N.F. Wang, B.H. Niu, L. Zhou, Y. Zheng, Enhanced adsorption of three fluoroquinolone antibiotics using polypyrrole functionalized *Calotropis gigantea* fiber, *Colloids Surf., A*, 574 (2019) 178–187.
- [175] R.N. Li, Z.W. Wang, J.L. Guo, Y. Li, H.Y. Zhang, J.M. Zhu, X.Y. Xie, Enhanced adsorption of ciprofloxacin by KOH modified biochar derived from potato stems and leaves, *Water Sci. Technol.*, 77 (2018) 1127–1136.
- [176] Y. Zhuang, F. Yu, J. Ma, Enhanced adsorption and removal of ciprofloxacin on regenerable long TiO_2 nanotube/graphene oxide hydrogel adsorbents, *Nanomaterials*, 2015 (2015) 8, doi: 10.1155/2015/675862.
- [177] P. Hongsawat, P. Prarat, C. Ngamcharussrivichai, P. Punyapalakul, Adsorption of ciprofloxacin on surface functionalized superparamagnetic porous silicas, *Desal. Water Treat.*, 52 (2014) 4430–4443.
- [178] F. Nekouei, S. Nekouei, H. Noorizadeh, Enhanced adsorption and catalytic oxidation of ciprofloxacin by an $\text{Ag}/\text{AgCl}@\text{N}$ -doped activated carbon composite, *J. Phys. Chem. Solids*, 114 (2018) 36–44.

- [179] S.T. Danahoglu, S.S. Bayazit, O.K. Kuyumcu, M.A. Salam, Efficient removal of antibiotics by a novel magnetic adsorbent: magnetic activated carbon/chitosan (MACC) nanocomposite, *J. Mol. Liq.*, 240 (2017) 589–596.
- [180] Y. Hu, Y. Zhu, Y. Zhang, T. Lin, G.M. Zeng, S.Y. Zhang, Y.R. Wang, W.Z. He, M.J. Zhang, H. Long, An efficient adsorbent: simultaneous activated and magnetic ZnO doped biochar derived from camphor leaves for ciprofloxacin adsorption, *Bioresour. Technol.*, 288 (2019) 121511, doi: 10.1016/j.biortech.2019.121511.
- [181] M.G. Sausen, F.B. Scheufele, H.J. Alves, M.G.A. Vieira, M.G.C. da Silva, F.H. Borba, C.E. Borba, Efficiency maximization of fixed-bed adsorption by applying hybrid statistical-phenomenological modeling, *Sep. Purif. Technol.*, 207 (2018) 477–488.
- [182] L. Wang, G.C. Chen, C. Ling, J.F. Zhang, K. Szerlag, Adsorption of ciprofloxacin on to bamboo charcoal: effects of pH, salinity, cations, and phosphate, *Environ. Prog. Sustainable Energy*, 36 (2017) 1108–1115.
- [183] S.E. Moradi, A.M.H. Shabani, S. Dadfarmia, S. Emami, Effective removal of ciprofloxacin from aqueous solutions using magnetic metal-organic framework sorbents: mechanisms, isotherms and kinetics, *J. Iran Chem. Soc.*, 13 (2016) 1617–1627.
- [184] C.R. Gadipelly, K.V. Marathe, V.K. Rathod, Effective adsorption of ciprofloxacin hydrochloride from aqueous solutions using metal-organic framework, *Sep. Sci. Technol.*, 53 (2018) 2826–2832.
- [185] W. Wang, J.D. Cheng, J. Jin, Q. Zhou, Y. Ma, Q.Q. Zhao, A.M. Li, Effect of humic acid on ciprofloxacin removal by magnetic multifunctional resins, *Sci. Rep.*, 6 (2016) 10, doi: 10.1038/srep30331.
- [186] X.N. Li, W.Q. Wang, J. Dou, J.S. Gao, S. Chen, X. Quan, H.M. Zhao, Dynamic adsorption of ciprofloxacin on carbon nanofibers: quantitative measurement by in situ fluorescence, *J. Water Process Eng.*, 9 (2016) 14–20.
- [187] Y.Z. Fu, Z.L. Yang, Y.C. Xia, Y.W. Xing, X.H. Gui, Adsorption of ciprofloxacin pollutants in aqueous solution using modified waste grapefruit peel, *Energy Sources Part A*, 43 (2019) 225–234.
- [188] C. Deb, B. Thawani, S. Menon, V. Gore, V. Chellappan, S. Ranjan, M. Ganapillai, Design and analysis for the removal of active pharmaceutical residues from synthetic wastewater stream, *Environ. Sci. Pollut. Res.*, 26 (2019) 18739–18751.
- [189] M.F. Li, Y.G. Liu, S.B. Liu, D. Shu, G.M. Zeng, X.J. Hu, X.F. Tan, L.H. Jiang, Z.L. Yan, X.X. Cai, Cu(II)-influenced adsorption of ciprofloxacin from aqueous solutions by magnetic graphene oxide/nitrilotriacetic acid nanocomposite: competition and enhancement mechanisms, *Chem. Eng. J.*, 319 (2017) 219–228.
- [190] J.A. González, J.G. Bafico, M.E. Villanueva, S.A. Giorgieri, G.J. Copello, Continuous flow adsorption of ciprofloxacin by using a nanostructured chitin/graphene oxide hybrid material, *Carbohydr. Polym.*, 188 (2018) 213–220.
- [191] Z.W. Zeng, S.R. Tian, Y.G. Liu, X.F. Tan, G.M. Zeng, L.H. Jiang, Z.H. Yin, N. Liu, S.B. Liu, J. Li, Comparative study of rice husk biochars for aqueous antibiotics removal, *J. Chem. Technol. Biotechnol.*, 93 (2018) 1075–1084.
- [192] Y.J. Kan, Q.Y. Yue, B.Y. Gao, Q. Li, Comparative study of dry-mixing and wet-mixing activated carbons prepared from waste printed circuit boards by NaOH activation, *RSC Adv.*, 5 (2015) 105943–105951.
- [193] J. Zhao, G.W. Liang, X.L. Zhang, X.W. Cai, R.N. Li, X.Y. Xie, Z.W. Wang, Coating magnetic biochar with humic acid for high efficient removal of fluoroquinolone antibiotics in water, *Sci. Total Environ.*, 688 (2019) 1205–1215.
- [194] X.M. Xu, Y.X. Liu, T. Wang, H.D. Ji, L. Chen, S. Li, W. Liu, Co-adsorption of ciprofloxacin and Cu(II) onto titanate nanotubes: speciation variation and metal-organic complexation, *J. Mol. Liq.*, 292 (2019) 111375, doi: 10.1016/j.molliq.2019.111375.
- [195] X.Y. Liu, M.Y. Liu, L. Zhang, Co-adsorption and sequential adsorption of the co-existence four heavy metal ions and three fluoroquinolones on the functionalized ferromagnetic 3D NiFe₂O₄ porous hollow microsphere, *J. Colloid Interface Sci.*, 511 (2018) 135–144.
- [196] W.Z. Duan, N.F. Wang, W.L. Xiao, Y.F. Zhao, Y. Zheng, Ciprofloxacin adsorption onto different micro-structured tourmaline, halloysite and biotite, *J. Mol. Liq.*, 269 (2018) 874–881.
- [197] X. Zhu, D.C.W. Tsang, F. Chen, S.Y. Li, X. Yang, Ciprofloxacin adsorption on graphene and granular activated carbon: kinetics, isotherms, and effects of solution chemistry, *Environ. Technol.*, 36 (2015) 3094–3102.
- [198] E.S.I. El-Shafey, H. Al-Lawati, A.S. Al-Sumri, Ciprofloxacin adsorption from aqueous solution onto chemically prepared carbon from date palm leaflets, *J. Environ. Sci.*, 24 (2012) 1579–1586.
- [199] Y.Y. Sun, H. Li, G.C. Li, B.Y. Gao, Q.Y. Yue, X.B. Li, Characterization and ciprofloxacin adsorption properties of activated carbons prepared from biomass wastes by H₃PO₄ activation, *Bioresour. Technol.*, 217 (2016) 239–244.
- [200] V.P. Singh, R. Vaish, Candle soot coated polyurethane foam as an adsorbent for removal of organic pollutants from water, *Eur. Phys. J. Plus*, 134 (2019), doi: 10.1140/epjp/i2019-12778-7.
- [201] E.C. Ngeno, V.O. Shikuku, F. Orata, L.D. Baraza, S.J. Kimosop, Caffeine and ciprofloxacin adsorption from water onto clinoptilolite: linear isotherms, kinetics, thermodynamic and mechanistic studies, *S. Afr. J. Chem.*, 72 (2019) 136–142.
- [202] S.L. Wu, Y.H. Li, X.D. Zhao, Q.J. Du, Z.H. Wang, Y.Z. Xia, L.H. Xia, Biosorption behavior of ciprofloxacin onto *Enteromorpha prolifera*: isotherm and kinetic studies, *Int. J. Phytorem.*, 17 (2015) 957–961.
- [203] F.A. Adekola, H.I. Adegoke, G.B. Adebayo, I.O. Abdulsalam, Batch sorption of ciprofloxacin on kaolinitic clay and hematite composite: equilibrium and thermodynamics studies, *Morocco J. Chem.*, 4 (2016) 384–.
- [204] X.M. Peng, F.P. Hu, T. Zhang, F.X. Qiu, H.L. Dai, Amine-functionalized magnetic bamboo-based activated carbon adsorptive removal of ciprofloxacin and norfloxacin: a batch and fixed-bed column study, *Bioresour. Technol.*, 249 (2018) 924–934.
- [205] P. Singla, N. Goel, S. Singhal, Affinity of boron nitride nanomaterials towards antibiotics established by exhaustive experimental and theoretical investigations, *Chem. Eng. J.*, 299 (2016) 403–414.
- [206] O.A. Attallah, M.A. Al-Ghobashy, M. Nebsen, M.Y. Salem, Adsorptive removal of fluoroquinolones from water by pectin-functionalized magnetic nanoparticles: process optimization using a spectrofluorimetric assay, *ACS Sustainable Chem. Eng.*, 5 (2017) 133–145.
- [207] Y. Fei, L. Yong, H. Sheng, M. Jie, Adsorptive removal of ciprofloxacin by sodium alginate/graphene oxide composite beads from aqueous solution, *J. Colloid Interface Sci.*, 484 (2016) 196–204.
- [208] S.K. Bajpai, N. Chand, M. Mahendra, The adsorptive removal of a cationic drug from aqueous solution using poly(methacrylic acid) hydrogels, *Water SA*, 40 (2014) 49–56.
- [209] Y.J. Chen, T. Lan, L.C. Duan, F.H. Wang, B. Zhao, S.T. Zhang, W. Wei, Adsorptive removal and adsorption kinetics of fluoroquinolone by nano-hydroxyapatite, *PLoS One*, 10 (2015) e0145025, doi: 10.1371/journal.pone.0145025.
- [210] F. Yu, S.N. Sun, S. Han, J. Zheng, J. Ma, Adsorption removal of ciprofloxacin by multi-walled carbon nanotubes with different oxygen contents from aqueous solutions, *Chem. Eng. J.*, 285 (2016) 588–595.
- [211] L.H. Huang, M. Wang, C.X. Shi, J. Huang, B. Zhang, Adsorption of tetracycline and ciprofloxacin on activated carbon prepared from lignin with H₃PO₄ activation, *Desal. Water Treat.*, 52 (2014) 2678–2687.
- [212] L. Chen, R. Ni, T. Yuan, Y. Gao, W. Kong, P. Zhang, Q.Y. Yue, B.Y. Gao, Effects of green synthesis, magnetization, and regeneration on ciprofloxacin removal by bimetallic nZVI/Cu composites and insights of degradation mechanism, *J. Hazard. Mater.*, 382 (2020) 121008, doi: 10.1016/j.jhazmat.2019.121008.

- [213] L.S. Chen, T.J. Yuan, R. Ni, Q.Y. Yue, B.Y. Gao, Multivariate optimization of ciprofloxacin removal by polyvinylpyrrolidone stabilized NZVI/Cu bimetallic particles, *Chem. Eng. J.*, 365 (2019) 183–192.
- [214] S. Ganesan, M. Amirthalingam, P. Arivalagan, S. Govindan, S. Palanisamy, A.P. Lingassamy, V.K. Ponnusamy, Absolute removal of ciprofloxacin and its degraded byproducts in aqueous solution using an efficient electrochemical oxidation process coupled with adsorption treatment technique, *J. Environ. Manage.*, 245 (2019) 409–417.
- [215] F. Nekouei, S. Nekouei, H. Kargarzadeh, Enhanced adsorption and catalytic oxidation of ciprofloxacin on hierarchical CuS hollow nanospheres@N-doped cellulose nanocrystals hybrid composites: kinetic and radical generation mechanism studies, *Chem. Eng. J.*, 335 (2018) 567–578.
- [216] D.N. Shan, S.B. Deng, C.X. Jiang, Y. Chen, B. Wang, Y.J. Wang, J. Huang, G. Yu, M.R. Wiesner, Hydrophilic and strengthened 3D reduced graphene oxide/nano- Fe_3O_4 hybrid hydrogel for enhanced adsorption and catalytic oxidation of typical pharmaceuticals, *Environ. Sci. Nano*, 5 (2018) 1650–1660.
- [217] L. Li, X. Zheng, Y. Chi, Y. Wang, X. Sun, Q. Yue, B.Y. Gao, S.P. Xu, Molecularly imprinted carbon nanosheets supported TiO_2 : strong selectivity and synergic adsorption–photocatalysis for antibiotics removal, *J. Hazard. Mater.*, 383 (2019) 121211, doi: 10.1016/j.jhazmat.2019.121211.
- [218] T.S. Anirudhan, J.R. Deepa, Nano-zinc oxide incorporated graphene oxide/nanocellulose composite for the adsorption and photocatalytic degradation of ciprofloxacin hydrochloride from aqueous solutions, *J. Colloid Interface Sci.*, 490 (2017) 343–356.
- [219] P.P. Zhao, F. Yu, R.Y. Wang, Y. Ma, Y.Q. Wu, Sodium alginate/graphene oxide hydrogel beads as permeable reactive barrier material for the remediation of ciprofloxacin-contaminated groundwater, *Chemosphere*, 200 (2018) 612–620.
- [220] M. Sharma, G. Singh, R. Vaish, Diesel soot coated non-woven fabric for oil-water separation and adsorption applications, *Sci. Rep.*, 9 (2019) 1–11.
- [221] F. Maraschi, A. Speltini, M. Sturini, L. Consoli, A. Porta, A. Profumo, Evaluation of rice husk for SPE of fluoroquinolones from environmental waters followed by UHPLC-HESI-MS/MS, *Chromatographia*, 80 (2017) 577–583.
- [222] N. Wang, Y.F. Wang, A.M. Omer, X.K. Ouyang, Fabrication of novel surface-imprinted magnetic graphene oxide-grafted cellulose nanocrystals for selective extraction and fast adsorption of fluoroquinolones from water, *Anal. Bioanal. Chem.*, 409 (2017) 6643–6653.
- [223] N. Dhiman, N. Sharma, Removal of pharmaceutical drugs from binary mixtures by use of ZnO nanoparticles, *Environ. Technol. Innovation*, 15 (2019) 100392, doi: 10.1016/j.eti.2019.100392.
- [224] A. Parpounas, V. Litskas, E. Hapeshi, C. Michael, D. Fattakassinos, Assessing the presence of enrofloxacin and ciprofloxacin in piggery wastewater and their adsorption behaviour onto solid materials, with a newly developed chromatographic method, *Environ. Sci. Pollut. Res. Int.*, 24 (2017) 23371–23381.
- [225] S.K. Bajpai, M. Bajpai, N. Rai, Sorptive removal of ciprofloxacin hydrochloride from simulated wastewater using sawdust: kinetic study and effect of pH, *Water SA*, 38 (2012) 673–682.
- [226] I.E. Touahar, L. Haroune, S. Ba, J.P. Bellenger, H. Cabana, Characterization of combined cross-linked enzyme aggregates from laccase, versatile peroxidase and glucose oxidase, and their utilization for the elimination of pharmaceuticals, *Sci. Total Environ.*, 481 (2014) 90–99.
- [227] C. De Oliveira Carvalho, D.L. Costa Rodrigues, E.C. Lima, C. Santanna Umpierrez, D.F. Caicedo Chaguezac, F. Machado Machado, Kinetic, equilibrium, and thermodynamic studies on the adsorption of ciprofloxacin by activated carbon produced from Jeriva (*Syagrus romanzoffiana*), *Environ. Sci. Pollut. Res. Int.*, 26 (2019) 4690–4702.
- [228] S. Aydin, M.E. Aydin, F. Beduk, A. Ulvi, Removal of antibiotics from aqueous solution by using magnetic Fe_3O_4 /red mud-nanoparticles, *Sci. Total Environ.*, 670 (2019) 539–546.
- [229] F.P. Zhao, E. Repo, D.L. Yin, L. Chen, S. Kalliola, J.T. Tang, E. Iakovleva, K.C. Tam, M. Sillanpää, One-pot synthesis of trifunctional chitosan-EDTA- β -cyclodextrin polymer for simultaneous removal of metals and organic micropollutants, *Sci. Rep.*, 7 (2017) 14.
- [230] K. Wang, D.D. Gao, J.R. Xu, L. Cai, J.R. Cheng, Z.X. Yu, Z.H. Hu, J. Yu, Interaction of ciprofloxacin with the activated sludge of the sewage treatment plant, *Environ. Sci. Pollut. Res.*, 25 (2018) 35064–35073.
- [231] R. Malik, A. Goyal, S. Yadav, N. Gupta, N. Goel, A. Kaushik, V. Kumar, K.B. Tikoo, S. Singhal, Functionalized magnetic nanomaterials for rapid and effective adsorptive removal of fluoroquinolones: comprehensive experimental cum computational investigations, *J. Hazard. Mater.*, 364 (2019) 621–634.
- [232] L. Garcia-Sanchez, T. Gutierrez-Macias, E.B. Estrada-Arriaga, Assessment of a *Ficus benjamina* wood chip-based aerated biofilter used for the removal of metformin and ciprofloxacin during domestic wastewater treatment, *J. Chem. Technol. Biotechnol.*, 94 (2019) 1870–1879.
- [233] X.B. Min, W. Li, Z.S. Wei, R. Spinney, D.D. Dionysiou, Y.W. Seo, C.-J. Tang, Q.Z. Tang, Q.Z. Li, R.Y. Xiao, Sorption and biodegradation of pharmaceuticals in aerobic activated sludge system: a combined experimental and theoretical mechanistic study, *Chem. Eng. J.*, 342 (2018) 211–219.
- [234] N. Dorival-Garcia, A. Zafra-Gomez, A. Navalon, J. Gonzalez, J.L. Vilchez, Removal of quinolone antibiotics from wastewaters by sorption and biological degradation in laboratory-scale membrane bioreactors, *Sci. Total Environ.*, 442 (2013) 317–328.
- [235] Y.Y. Jia, H.Q. Zhang, S.K. Khanal, L.W. Yin, H. Lu, Insights into pharmaceuticals removal in an anaerobic sulfate-reducing bacteria sludge system, *Water Res.*, 161 (2019) 191–201.
- [236] L. Wang, Z.M. Qiang, Y.G. Li, W.W. Ben, An insight into the removal of fluoroquinolones in activated sludge process: sorption and biodegradation characteristics, *J. Environ. Sci.*, 56 (2017) 263–271.
- [237] H.Q. Zhang, S.K. Khanal, Y.Y. Jia, S.L. Song, H. Lu, Fundamental insights into ciprofloxacin adsorption by sulfate-reducing bacteria sludge: mechanisms and thermodynamics, *Chem. Eng. J.*, 378 (2019) 122103, doi: 10.1016/j.cej.2019.122103.
- [238] W. Mekhamer, S. Al-Tamimi, Removal of ciprofloxacin from simulated wastewater by pomegranate peels, *Environ. Sci. Pollut. Res. Int.*, 26 (2019) 2297–2304.
- [239] M. Khoder, N. Tsapis, H. Huguet, M. Besnard, C. Gueutin, E. Fattal, Removal of ciprofloxacin in simulated digestive media by activated charcoal entrapped within zinc-pectinate beads, *Int. J. Pharm.*, 379 (2009) 251–259.
- [240] F.K. Mostafapour, D. Balarak, M. Baniasadi, Removal of ciprofloxacin from pharmaceutical wastewater by adsorption on SiO_2 nanoparticle, *J. Pharm. Res. Int.*, 25 (2018) 1–9.
- [241] S. Alvarez-Torrellas, J.A. Peres, V. Gil-Alvarez, G. Ovejero, J. Garcia, Effective adsorption of non-biodegradable pharmaceuticals from hospital wastewater with different carbon materials, *Chem. Eng. J.*, 320 (2017) 319–329.
- [242] A. Gupta, A. Garg, Adsorption and oxidation of ciprofloxacin in a fixed bed column using activated sludge derived activated carbon, *J. Environ. Manage.*, 250 (2019) 109474, doi: 10.1016/j.jenvman.2019.109474.
- [243] D. Balarak, A.H. Mahvi, M.J. Shim, S.M. Lee, Adsorption of ciprofloxacin from aqueous solution onto synthesized NiO: isotherm, kinetic and thermodynamic studies, *Desal. Water Treat.*, 212 (2021) 390–400.
- [244] D. Balarak, G. McKay, Utilization of MWCNTs/ Al_2O_3 as adsorbent for ciprofloxacin removal: equilibrium, kinetics and thermodynamic studies, *J. Environ. Sci. Health A*, 56 (2021) 324–333.
- [245] T.J. Al-Musawi, A.H. Mahvi, A.D. Khatibi, D. Balarak, Effective adsorption of ciprofloxacin antibiotic using powdered activated carbon magnetized by iron(III) oxide magnetic nanoparticles, *J. Porous Mater.*, 28 (2021) 835–852.